ISTANBUL TECHNICAL UNIVERSITY ★ GRADUATE SCHOOL OF SCIENCE ENGINEERING AND TECHNOLOGY

ELECTROSPUN NANOFIBERS OF POLY(BUTYL ACRYLATE-CO-METHYL METHACRYLATE)/POLYPYRROLE COMPOSITES

M.Sc. THESIS

Derya AKÇÖREN

Department of Polymer Science and Technology

Polymer Science and Technology Programme

Thesis Advisor: Prof. Dr. A. Sezai SARAÇ

JANUARY 2013

ISTANBUL TECHNICAL UNIVERSITY ★ GRADUATE SCHOOL OF SCIENCE ENGINEERING AND TECHNOLOGY

ELECTROSPUN NANOFIBERS OF POLY(BUTYL ACRYLATE-CO-METHYL METHACRYLATE)/POLYPYRROLE COMPOSITES

M.Sc. THESIS

Derya AKÇÖREN

(515091047)

Department of Polymer Science and Technology

Polymer Science and Technology Programme

Thesis Advisor: Prof. Dr. A. Sezai SARAÇ

JANUARY 2013

İSTANBUL TEKNİK ÜNİVERSİTESİ ★ FEN BİLİMLERİ ENSTİTÜSÜ

ELEKTROSPUN YÖNTEMİ İLE POLİ(BUTİL AKRİLAT-KO-METİL METAKRİLAT)/POLİPİROL KOMPOZİTLERİN ELDE EDİLMESİ

YÜKSEK LİSANS TEZİ

Derya AKÇÖREN
(515091047)

Polimer Bilim ve Teknolojileri

Polimer Bilim ve Teknolojileri Programı

Tez Danışmanı: Prof. Dr. A. Sezai SARAÇ

OCAK 2013

Derya AKÇÖREN a M.Sc Student of ITU **Institute of Science and Technology/Graduate School of Istanbul Technical University student** ID 515091047, succesfully defended the **thesis** entitled **"ELECTROSPUN NANOFIBERS OF POLY(BUTYL ACRYLATE-CO-METHYL METHACRYLATE)/POLYPYRROLE COMPOSITES"**, which she prepared after fulfiling the requirements specified in the associated legislations, before the jury whose signatures are below.

Thesis Advisor :	**Prof. Dr. A.Sezai SARAÇ** İstanbul Technical University	.....
Jury Members :	**Prof. Dr. Ahmet AKAR** Istanbul Technical University	.....
	Prof. Dr. Hale KARAKAŞ Istanbul Technical University	.....

Date of Submission : 17 December 2012

Date of Defense : 21 January 2013

To my family,

FOREWORD

I would like to express my gratitude to my thesis supervisor, Prof. Dr. A.Sezai SARAÇ for his continuous encouragement, guidance, helpful critics and discussions in my studies.

I would like to give my personal thanks to Merih Zeynep AVCI. This thesis was impossible without her guidance and help.

I would like to give my special thanks to my laboratory friends Timucin BALKAN, Burcu ARMAN, Aslı GENÇTÜRK, Selda ŞEN, Başak DEMİRCİOĞLU, Kezban HÜNER, Tolga SATICI, Diğdem GİRAY, Nazif Uğur KAYA, Hacer DOLAŞ, İlknur GERGİN, Fatma Gül GÜLER, Suat ÇETİNER, Bilge KILIÇ, Ezgi İŞMAR, Yasemin YERLİKAYA for their collaborative and friendly manner.

I would like thanks to my collegues Gözde ÖZKARAMAN, Seher UZUNSAKAL, Selim ZEYDANLI, Merve ZAKUT, Bilge CEBISLI, Fatma CÖMERT, Neşe ÇAKIR, Mehmet BASDAL, Ömer Faruk VURUR, Merve Çetin MOCANTAŞ and Damla GÜLFİDAN from Istanbul Technical University.

I would like to thank my dear friends Melahat ŞAHİN and Göker ZAFER for their special friendships. Their point of view to life had taught me a lot of thing.

I would like to thanks Murat YÜCEL and BSH Home Appliances business friends who always encouraged ne during my studies.

My personal thanks goes to my love Dinçay AKÇÖREN for his full support, patience, understanding and being always with me during these seven years.

Most of all, I would like to thanks my family, especially my mother Rezzan ÇETECİOĞLU, my father Ali Rıza ÇETECİOĞLU, my sister Deniz ÇETECİOĞLU, my aunt Fidan ÇETECİOĞLU and my cousin Zeynep ÇETECİOĞLU. For all those times they stood by me and heartedly supported. I was able to accomplish everything in my life thanks to their eternal love.

Finally, I would like to thank all of my other friends for all their emotional assists and motivation during this extremely difficult accomplishment.

December 2012

Derya AKÇÖREN
(Chemical Engineer)

TABLE OF CONTENT

Page

ABBREVIATIONS

BA	**:** Butyl Acrylate
MMA	**:** Methyl Methacrylate
DMF	**:** Dimethylformamide
DSC	**:** Differential Scanning Calorimetry
FTIR-ATR	**:** Fourier Transform Infrared Spectroscopy
GPC	**:** Gel Permeation Chromatography
KPS	**:** Potassium Peroxydisulfate
M_n	**:** Number Average Molecular Weight
M_v	**:** Viscosity Average Molecular Weight
M_w	**:** Weight Average Molecular Weight
NMR	**:** Nucleear Magmetic Resonance
PDI	**:** Polydispersity Index
PMMA	**:** Poly (methyl methacrylate)
P(BA-co-MMA)	**:** Poly Butyl Acrylate-Methyl Methacrylate Copolymer
P(BA-co-MMA) @PPy$_{1\text{-}2\text{-}3\text{-}4}$	**:** Composites in different Py feed mole fraction: 10%, 20%, 30%, 40%
SDS	**:** Sodium Dodecyl Sulfate
SEM	**:** Scanning Electron Microscopy
T_g	**:** Glass Transition Temperature
η	**:** Intrinsic Viscosity
ε	**:** Dielectric Constant
θ^o	**:** Contact Angle
DMA	**:** Dynamic Mechanical Analyser
PPy	**:** Polypyrrole

LIST OF TABLES

Page

LIST OF FIGURES

Page

ELECTROSPUN NANOFIBERS OF POLY(BUTYL ACRYLATE–co-METHYL METHACRYLATE)/POLYPYRROLE COMPOSITES

SUMMARY

This study can be categorized into two parts. The first part aims to synthesis new polymeric nanocomposite materials which can be used for electromagnetic interference shielding and absorbent panel applications. In the first part of this study, nanofibers of n-Butyl Acrylate/Methyl Methacrylate copolymer are synthesized by electrospinning method. Emulsion polymerization of n-Butyl Acrylate (BA) and Methyl Methacrylate (MMA) initiated by Potassium Persulfate (KPS) in the aqeuos medium was performed. Sodium Dodecyl Sulphate was used as emulsifier. Effects of solutions properties and processing conditions on the electrospun nanofiber morphology were investigated. Afterwards, composites were characterized in terms of chemical composition, surface morphology, particle size, conductivity, thermal and mechanical properties by using Dynamic Mechanical Analyser (DMA), Fourier Transform Infrared - Attenuated Total Reflectance spectrophotometer (FTIR-ATR), Scanning Electron Microscope (SEM), Gel Permeation Chromatography (GPC), Contact Angle Meter, Nuclear Magnetic Resonance Spectrometer (NMR).

The second aim was to obtain P(BA-co-MMA)/ PPy based nanofibers for use new generation products such as electrostatic discharge, sensors application in textile industry. Pyrrole (Py) was polymerized on P(BA-co-MMA) matrix in dimethylformamide (DMF). Ammonium Cerium (IV) Nitrate salt was used as an oxidant for both copolymer formation and polymerization of Py on P(BA-co-MMA) matrix. P(BA-co-MMA)/PPy composites were obtained by adding the pyrrole monomers into the continued reaction. Nanofibers were obtained from this solution by electrospinning method.

PPy ring vibration was increased on P(BA-co-MMA) composites by addition of pyrrole which was occured at 1448 cm^{-1} proved by FTIR-ATR analysis. A linear relationship was determined between the absorbance ratios of functional groups corresponding to the conjugated polymeric units and initial Py concentration.

Scanning electron microscope images indicated that the diameters of nanofibers were dependent on PPy content and that the average nanofiber diameters were reduced by increasing the initially added Py content. The contact angle measurements indicated that the

Electrospun nanofiber copolymers were high hydrophobic with addition of pyrrole which had a water contact angle of 152^{o}. The influence of the pyrrole content on the dielectric permittivity, dielectric loss and electrical properties of the composite films were analyzed in the frequency range from 0.01 Hz to 10 MHz. By the increase in the amount of pyrrole in the composite film, AC conductivity, dielectric constants

and dielectric loss increased. Conducting nanofibers were evaluated by UV-Visible spectrometer and Novocontrol Broadband Dielectric Spectrometer .

ELEKTROSPUN YÖNTEMİ İLE POLİ(BUTİL AKRİLAT-ko-METİL METAKRİLAT)/POLİPİROL KOMPOZİTLERİN ELDE EDİLMESİ

ÖZET

Bu çalışmada butil akrilat (BA) ve metil metakrilat (MMA) kopolimerleri sentezlenmiş ve karakterizasyonları yapılmıştır. Sentezlenen kopolimerler elektroçekim ile nanolif üretiminde kullanılmıştır. Sentezlenen kopolimere artan oranlarda pirol eklenmiştir. Polimerizasyon sonucunda poli(butil akrilat-ko-metil metakrilat)/polipirol kompozitleri elde edilmiştir. Bu çalışmanın hedefi kopolimerlerden nanolif üretilmesi ve üretilen nanoliflerin iletkenliklerinin kanıtlanmasıdır.

Bu calışma iki kısıma ayrılabilir. İlk kısım yeni polimerik nanokompozit malzemelerin sentezlenmesini amaçlanmaktadır. Butil akrilat (BA) ve metil metakrilat (MMA) monomerleri çözücünün su olduğu ortama eklenmiştir. Monomer fazını dağıtabilmek için emülsifiyar eklenmiştir. Ortama başlatıcı eklenerek emülsiyon polimerizasyonu başlamıştır. Kopolimeri sentezlemek için gerekli olan reaksiyon süresi 3 saat ve 70 C'dir. Sulu ortamda potasyum persülfat ile başlatılan Butil Akrilat (BA) ve Metil Metakrilat (MMA) emülsiyon polimerizasyonu yapılmıştır. Sodyum Dodesil Sülfat emülsifiyar olarak kullanılmıştır. Üç saat süren kopolimerizasyon sonucunda reaksiyon sonlandırılarak; suda çökelek halinde kopolimer elde edilmiştir. Kopolimerler etanol ile yıkandıktan sonra vakum etüvünde kurutulmuştur. Çözelti özelliklerinin ve süreç koşullarının elektrospun morfolojisi üzerine olan etkileri incelenmiştir. Bu aşamalardan sonra, kompozitler kimyasal yapıları, yüzey morfolojileri, parçacık boyutları, iletkenlikeri ve mekanik özellikleri açılarından incelenmişlerdir. Bu incelemelerde DMA, FTIR-ATR, SEM, GPC ve NMR cihazları kullanılmıştır.

İlk kısımda, n-Butil Akrilat / Metil Metakrilat kopolimerler nanofiberleri elektrospin yöntemi ile elde edilmiştir. Butil akrilat metil metakrilat kopolimerinin spektroskopik, termal ve mekanik analizleri FTIR-ATR (Fourier Transform Kızılötesi-Azaltılmış Toplam Reflektans), NMR (Nükleer Manyetik Rezonans) spektrometre, DSC (Diferansiyel Taramalı Kalorimetre), DMA (Dinamik Mekanik Analiz), SEM (Taramalı Elektron Mikroskobu), UV (Görünür Bölge Absorpsiyon Spektrometresi) ile yapılmıştır.

Çalışmanın sonraki aşamasında poli(butil-ko-metilmetakrilat) kopolimerlerine farklı miktarlarda pirol eklenmiştir. Pirol monomeri seryum amonyum nitrat ile birlikte çözülmüş ve poli(butil-ko-metilmetakrilat) kopolimerlerine damla damla eklenmiştir. Yaklaşık 12 saat boyunca karıştırılmış ve etanol ile çöktürülmüştür. Yıkanan kompozit 24 saat boyunca etüvde kurutulmuştur. Elde edilen 4 farklı kompozit dimetil formaldid (DMF) içerisinde çözülmüştür. Hazırlanan çözeltilerden

elektroçekim yöntemiyle nanolifler hazırlanmıştır. Tüm kopolimerler için çözelti konsantrasyon, besleme hızı ve uzaklık gibi elektroçekim değişkenleri sabit tutularak polipirolün nanolif çapına etkisi incelenmiştir. Elektroçekim için çözeltiler kütlece %5 katı içerecek şeklinde hazırlanmıştır. Şırıngaya doldurulan kopolimer çözeltisi pompa ile 1 ml/saat debiyle beslenmiştir. Kopolimer çözeltileri için gerekli gerilim 15 kV olarak uygulanmıştır. Topraklama hattına bağlanmış metal plaka şırınganın ucundan 15 cm uzağa yerleştirilmiştir. Farklı besleme hızlarının kompozit liflerine etkisini incelemek için kompozit miktarları sahip tutularak elektrospin yapılmıştır. Besleme hızları; 1ml/saat, 3 ml/saat, 5ml/saat ve 7 ml/saat olarak değiştirilmiştir. Besleme hızı artırıldıkça nanolif çaplarında artış meydana gelmiştir. Nanolif eldesinde iletken polimerin etkisini incelemek amacıyla ağırlıkça %10, %20, %30 ve % 40 pirol girilmiştir. Nanofiber çaplarının polipirol miktarına bağlı olarak değiştiği taramalı elektron mikroskop görüntüleri ile gösterilmiştir. Ortalama nanolif çapları başlangıçta eklenen pirol miktarının artması ile azaldığı gösterilmiştir.

Taramalı Elektron Mikroskobu ile poli(butil-ko-metilmetakrilat) kopolimerlerinin lif çapı 600 ± 93 olarak ölçülmüştür. Ortalama nanolif çapları, polipirol artışına bağlı olarak 463 ± 51'den 263 ± 50'ye düştüğü görülmüştür.

Başka bir parametre olarak farklı çözücülerin lif çaplarına etkisi çalışılmıştır. Dimetil formaldehid (DMF), tetrahidrofuran (THF) ve farklı oranlarda dimetil formaldehid ile tetrahidrofuran karışımı hazırlanmıştır. Çözeltilerin sahip oldukları dielektrik sabitleriyle nanolif çaplarıyla olan ilişkisi araştırılmıştır. Buna göre dielektrik sabiti en yüksek olan DMF çözeltisi ile lif atıldığında kompozit en ince nanolif çapı elde etmiştir. En düşük dielektik sabitine sahip olan THF çözeltisi ile atıldığında ise en kalın nanolif çapı gözlenmiştir.

Çalışmanın ikinci bölümünde, elektrostatik deşarj, tekstil endüstrisinde sensör uygulamaları gibi yeni nesil ürünlerde kullanılmak üzere polipirol/poli(butil-ko-metilmetakrilat) tabanlı nanofiberler elde edilmesidir. Pirol (Py), P(BA-co-MMA) Poli(butil-ko-metilmetakrilat) matrisinde ve dimethylformamide (DMF) içerisinde polimerleştirilmiştir. Amonyum sezyum (IV) nitrat tuzu hem polimer formasyonu için hem de pirol polimerizasyonu için oksidant olarak kullanılmıştır. Devam eden reaksiyona pirol monomerleri eklenerek P(BA-co-MMA)/PPy kompozitleri elde edilmiştir.

Pirol eklenmesi ile kompozitlerle halka titreşimlerinin arttığı FTIR-ATR analizleri ile gösterilmiştir. Bu gruba ait pikin polipirol oluşumuna bağlı olarak başlangıçta eklenen pirol miktarı ile lineer bir ilişki olduğu belirlenmiştir. Absorbsiyon oranı ile konjuge polimer birimleri ve başlangıç pirol konsantrasyonu arasında doğrusal bir oran belirlenmiştir. Pirolun karakteristik piki olan C-N piki 1448 cm^{-1}, yapıya arttıkça artan absorbsiyonda görülmüştür. Ayrıca 1724 cm^{-1} ve 1144 cm^{-1} görülen C=O ve O-CH_3 pikleri polipirol yapıya girdikçe de artmaktadır.

UV görünür bölge spektrofotometresi ile kompozit yapılarında polipirol yapısı olduğu gözlenmiştir. Kopolimer yapısında polipirol miktarı arttıkça UV görünür bölgesinde öloçülen absorbans değeri artmaktadır. Bu durum homo lumo arasındaki π-π^* geçişlerdir.

Nükleer manyetik rezonans spektrumu (NMR) ölçümleri 250 MHz Bruker Aspect AC 3000 spektrometre cihazıyla yapılmıştır. Çözücü olarak $CDCL_3$ kullanılmıştır. Çözücünün karakteristik piki 7.24 ppm de çıkmıştır. NMR verilerine göre Poli(butil-

ko-metilmetakrilat) kopolimerinin yapısına polipirol girdiği görülmüştür. Polipirol halkasındaki hidrojen piki 8.0-8.1 ppm de görülmüştür. Bütil akrilata ait olan –O-CH_2 piki 3.99 ppm de görülmüştür, metil metakrilata ait olan –O-CH_3 piki 3.64 ppm de görülmüştür.

Elde edilen nanoliflerden KSV CAM 200 cihazı ile kontak açı ölçülmüştür. Kontak açı ölçümlerinin gösterdiği üzere polipirol eklendikçe nanofiber çapları incelmekte ve temas açıları artmaktadır. Temas açıları arttıkça yüksek hidrofobik özellik kazanmaktadır. En düşük polipirol miktarına sahip poli(butil-ko-metilmetakrilat) kopolimerinin açısı 122° iken en yüksek polipirola sahip olan poli(butil-ko-metilmetakrilat) ise 152° sahiptir. Polipirol miktarı Poli(butil-ko-metilmetakrilat) kopolimerininde arttıkça kompozitin hidrofobik özelliği artmıştır.

Polimerlerin dinamik mekanik özellikleri DMA (Dinamik Mekanik Analiz) cihazıyla ölçülmüştür. Poli(butil-ko-metilmetakrilat) kopolimerinin yapısına polipirol girdikçe kompozitin Tg'sinin düştüğü görülmüştür. En düşük polipirola sahip olan kompozitin en yüksek Tg'ye sahip olduğu görülmüştür.

Elektrik iletkenlikleri Novocontrol geniş-bantlı dielektrik spektroscopisinden ölçülmüştür. Poli(butil-ko-metilmetakrilat) Poli(butil-ko-metilmetakrilat)/polipirol kompozisyonlarından elde edilen polimerik film özellikleri artan polipirol iletken monomerinin iletkenlik üzerindeki etkisi araştırılmıştır. Yapıya giren polipirol miktarının, kompozit filmlerin dielektrik geçirgenliği, dielektrik kaybı ve elektriksel özellikleri üzerindeki etkisi 0.01 Hz ile 10 MHz frekans aralığında analiz edilmiştir. Polipirol miktarı arttıkça AC ilektenlik ve dielektrik sabiti ve dielektrik kaybının arttığı gözlemlenmiştir.

Yapılan çalışmalar sonucunda elde edilen nanofiberler çeşitli iletken giysi ve kumaşlarda uygulanabilinecektir. Tekstil endüstrisinde yeni nesil ürünlerde elektrostatik deşarj, sensor gibi uygulama alanlarında kullanılmak üzere tasarlanma olanağı bulunmaktadır.

1. INTRODUCTION

Conducting polymers are a new class of materials with an extensive delocalisation of p-electrons conjugated network opening the way to new applications in the fields of energy storage, microelectronics, textiles, sensors, electroluminescence and electromagnetic interference (EMI) shielding. The essential feature of the conducting polymers is the one of providing p bands of delocalised molecular orbital within which full range of semiconductors and metal behavior can be achieved through the control of the degree of band filling [1,2]. Among the conducting polymers, polypyrrole (PPy) has attracted much attention in particular due to its high conductivity, redox properties, good stability, environmental stability and easy preparation as a film or powder by both electrochemical and chemical methods under various conditions [3,4].

Development of textiles with new applications and properties has received great attention during the last years. One of these properties is the electrical conductivity in textiles. Development of textiles with new properties and applications has received great attention during the last years. One of these properties is the electrical conductivity in textiles. The reason is that electrostatic and electromagnetic interference became common place because of human lifestyle changes and the increasing sophistication of industrial technology [4,5].

Applications of conductive textiles are varied; like electromagnetic interference shielding, electrostatic dissipating, antistatic applications, gas sensors, biomechanical sensors, heating devices, flooring, microwave reduction. The microwave absorption characteristics of conductive textiles are highly desirable, allowing these materials to be used in military applications such as radar protective fabrics [6,7]. EMI shielding performance can be controlled by varying the electrical conductivities and dielectric constants [7-9]. In the case of a conducting composite prepared by the simple coating of conducting polymers onto the surface of the matrix polymer, any interaction between the two components usually does not exist [10].

In this study, firstly emulsion polymerization of n-Butyl Acrylate (BA) and Methyl Methacrylate (MMA) initiated by Potassium Peroxydisulfate (KPS) in the aqeuos medium was performed. By using electrospining method, electrospun nanofibers of P(BA-co-MMA) are first obtained. Second part of study pyrrole (Py) was polymerized on P(BA-co-MMA) matrix in dimethylformamide (DMF). Nanofibers contact angles were measurement with use the electrospun mats. The effect of the PPy content on the resulting nanofiber composites is characterized by spectroscopic, morphological, and thermal measurement methods. Nanofibers were were investigated in terms of chemical composition, surface morphology, particle size, conductivity, thermal and mechanical properties by using DMA, Fourier Transform Infrared - Attenuated Total Reflectance spectrophotometer (FTIR-ATR), Scanning Electron Microscope (SEM), nuclear magnetic resonance spectrometer (NMR). The second part of this study, the electrospinning method was applied to produce nanofibers of P(BA-co-MMA)/PPy composite.

2. THEORETICAL PART

2.1 Polyacrylates

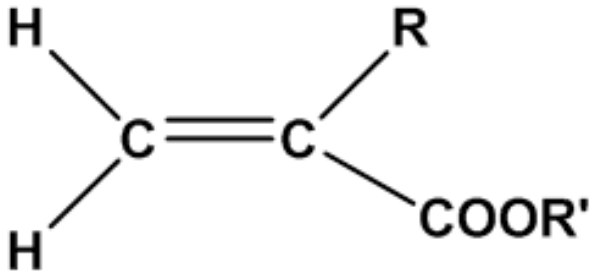

Figure 2.1: General Formula of Acrylates

Acrylate monomers used to form acrylate polymers are based on the structure of acrylic acid, which consists of a vinyl group and a carboxylic acid terminus. Other typical acrylate monomers are derivatives of acrylic acid, such as methyl methacrylate in which one vinyl hydrogen and the carboxylic acid hydrogen are both replaced by methyl groups, and acrylonitrile in which the carboxylic acid group is replaced by the related nitrile group.

Polyacrylate is a chemical class of acrylate polymers derived from the polymerization of acrylic acid esters and salts. Each acrylate monomer contains a vinyl group: a pair of double-bonded carbon atoms attached to the carbon of a carboxyl group. Polyacrylates containing the R groups methyl (— CH_3), ethyl (— C_2H_5), n-butyl (—C_4H_9) and cyclohexyl (—CeH_{11}) are of the greatest industrial importance. These polyacrylates are transparent thermoplastic polymers that are physiologically harmless and readily soluble in organic solvents and are characterized by low resistance to oil and gasoline.

Polyacrylates are used in the production of organic glass (mainly polymethyl methacrylate), films, paints and varnishes, adhesives, and impregnation compositions for paper, leather, wood, and fabrics.

2.1.1 Areas of application

Polyacrylates are widely used in medicine, especially in dentistry, for the preparation of artificial jaws and teeth and for fillings. Acrylate polymers and copolymers are used to make prostheses and contact lenses, as well as special castings for preserving various items. Acrylates are widely used as co-monomers to increase the plasticity of rigid polymers and to produce acrylic rubbers.

2.2 Polymerization of Acrylates and Emulsion Polymerization

Emulsion polymerization involves the reaction of free radicals with relatively hydrophobic monomer molecules within submicron polymer particles dispersed in a continuous aqueous phase. This unique polymerization process that is heterogeneous in nature exhibits very different reaction mechanisms and kinetics compared to bulk or solution free radical polymerization. Surfactant is generally required to stabilize the colloidal system; otherwise, latex particles nucleated during the early stage of polymerization may experience significant coagulation in order to reduce the interfacial free energy. This feature may also come into play in determining the number of particles available for the consumption of monomer therein.

Advantages of emulsion polymerization include:

- The continuous water phase is an excellent conductor of heat and allows the heat to be removed from the system, allowing many reaction methods to increase their rate.
- Since polymer molecules are contained within the particles, viscosity remains close to that of water and is not dependent on molecular weight.
- The final product can be used as is and does not generally need to be altered or processed.

Most emulsion polymerizations use a free-radical polymerization method. Emulsion polymerization can be carried out as a batch reaction, but in many cases is performed as a starve-fed reaction to insure a good distribution of monomers into the polymer backbone chain. The leading theory for the mechanism of starve-fed, free-radical emulsion polymerization is summarized by the following:

- Surfactants emulsify the monomer in a water continuous phase.
- Excess surfactant creates micelles in the water.

- Small amounts of monomer diffuse through the water to the micelle.
- Initiator (water-soluble and introduced into the water phase) reacts with monomer in the micelles

The micelles in total, comprise a much larger surface area in the system than the fewer, larger monomer droplets, which is why the initiator typically reacts with the micelle and not the monomer droplet.

Monomer in the micelle quickly polymerizes and the growing chain terminates. More monomer from the droplets diffuses to the growing micelle/particle, where more initiators will eventually react. Monomer droplets and initiator are continuously, and slowly added to maintain their levels in the system as the particles grow. When the monomer droplets have been completely consumed, the initiator is typically added in for a little while longer to consume any residual monomer. The final product is a 'disperion' of polymer particles in water, it can also be known as a polymer colloid, a latex, or commonly and inaccurately as an 'emulsion'. Inaccurate because the final form is no longer an oil-phase solubilized in a continous phase, but rather finely dispersed discrete solid polymer particles [11].

In emulsion polymerization there are some key “ingredients”:

- The monomer must be insoluble in water and polymerizable by free radicals
- Water-soluble initiator
- Water
- Surfactant

2.2.1 Formation of micelles

When monomers of strongly polar "heads" and a non-polar chain "tails" are added to water, micelles are formed. The non-polar tails of the monomer molecules clump into the center of a ball like structure and the polar heads of the monomers present themselves for interaction with the water molecules on the outside of the micelle. Polymerization occurs when initiators migrate into the micelles, inducing the monomer molecules to form large molecules that make up the latex particle [12]. Figure 2.2 is a schematic representation of micelle nucleation model.

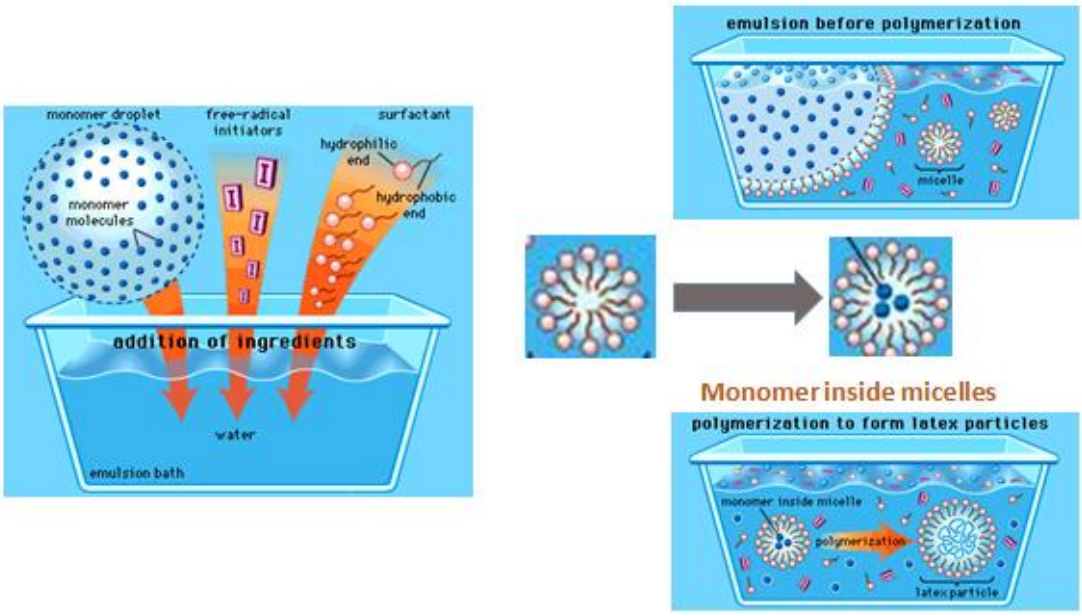

Figure 2.2: Schematic view of emulsion polymerization [12].

2.3 Free radical polymerization

Free Radical Polymerization has been a very important industrial process due to low requirements on monomer and reactant purity facile copolymerization and the fact that polymerization can be conducted in either emulsion or suspension using water as the medium. The polymers obtained via this method are used in the manufacture of numerous products such as fabrics surface coatings plastics paints packaging and contact lenses.

Free Radical Polymerization can be carried out under relatively undemanding conditions

- It exhibits a tolerance of trace impurities
- High molecular weight polymers can be produced without removal of the stabilizers present in commercial polymers.
- Trace amount of oxygen does not disturb the polymerization.
- Free radical reactions can be conducted in aqueous media.
- A variety of monomers can be polymerized via free radical polymerization route unlike to the ionic polymerization techniques.

Free Radical Polymerization is initiated by radicals propagated by macro-radicals. These radicals exhibit an unpaired electron. Initiating radicals are rarely formed by monomers themselves but rather thermally electrochemically or photo chemically from the homolytic chain cleavage of the deliberatly added initiators. Free Radical Polymerization is a chain growth reaction and traditionally consists of these main steps [13].

- Initiation: a reactive site is formed thereby initiating the polymerization
- Propagation: Once an initiator activates the polymerization monomer molecules are added one by one to the active chain end in the propagation step. The reactive site is regenarated after each addition of monomer.
- Transfer: occurs when an active site is transferred to an independent molecule such as monomer iniator polymer or solvent This process results in both a terminated molecule and a new active site that is capable of undergoing propagation.
- Termination: In this final step eradication of active sites leads to terminated or inert macromolecules. Termination occurs via coupling reactions of two centers referred to as combination or atomic transfer between active chains.

The free radical chain process is demonstrated schematically below R. represents a free radical capable of initiating propagation M denotes a molecule of monomer Rm and Rn refer to propagating radical chains with degrees of polymerization of m and n respectively, AB is a chain transfer agent and Pn+Pm represent terminated macromolecules. Because chain transfer may occur for every radical at any and all degrees of polymerization the influence of chain transfer on the average degree of polymerization and on polydispersity carries enormous consequences. Furthermore propagation is a first order reaction while termination is second order. Thus the proparation of termination to propagation increases substantial with increasing free radical concentrations. Chain transfer and termination are impossible to control in classical free radical processes a major downfall when control over polymerization is desired [14].

initiator $\longrightarrow$ $2R^{\cdot}$

$R^{\cdot}+M \longrightarrow R_1^{\cdot}$ chain initiator

$R_1^{\cdot} + nM \longrightarrow R_n^{\cdot}$ propagation

$R_n^{\cdot} + AB \longrightarrow R_{n\,A} + B^{\cdot}$ transfer

$R_m^{\cdot} + R_n^{\cdot} \longrightarrow P_{m+n}$ combination

$R_m^{\cdot} + R_n^{\cdot} \longrightarrow P_m + P_n$ disproportion

Some of the popular emulsions available in the market include Polyvinyl acetate homopolymers and copolymers, styrene butadiene latex, and acrylic emulsions. These emulsions find applications in adhesives, paints, paper coating and textile coatings. They are finding increasing acceptance and are preferred over solvent based products in these applications as a result of their eco friendly characteristics due to the absence of VOC (Volatile Organic Compounds) in them.

2.4 Monomers

Typical monomers are those that undergo radical polymerization, are liquid or gaseous at reaction conditions, and are poorly soluble in water. Solid monomers are difficult to disperse in water. If monomer solubility is too high, particle formation may not occur and the reaction kinetics reduce to that of solution polymerization. Ethylene and other simple olefins must be polymerized at very high pressures (up to 800 bar).

2.5 Comonomers

Copolymerization is common in emulsion polymerization. The same rules and comonomer pairs that exist in radical polymerization operate in emulsion polymerization. However, copolymerization kinetics are greatly influenced by the aqueous solubility of the monomers. Monomers with greater aqueous solubility will tend to partition in the aqueous phase and not in the polymer particle. They will not get incorporated as readily in the polymer chain as monomers with lower aqueous solubility. This can be avoided by a programmed addition of monomer using a semi-batch process. Small amounts of acrylic acid or other ionizable monomers are sometimes used to confer colloidal stability to a dispers.

2.6 Initiators

The initiators used in emulsion polymerization are water-soluble initiators such as potassium or ammonium persulfate, hydrogen peroxide, and 2,20-azobis(2-amidinopropane) dihydrochloride. Partially water-soluble peroxides such a succinic acid peroxide and t-butyl hydroperoxide and azo compounds such as 4,40-azobis(4-cyanopentanoic acid) have also been used. Redox systems such as persulfate with ferrous ion are commonly used. Redox systems are advantageous in yielding desirable initiation rates at temperatures below 50 C. Other useful redox systems include cumyl hydroperoxide or hydrogen peroxide with ferrous, sulfite, or bisulfite ion [15].

2.7 Polymeric Stabilizers

Typical polymeric stabilizers used for oil in water suspension polymerization reactions are poly(vinyl alcohol) co-(vinyl acetate) formed from the partial hydrolysis (80-90%) of polyvinyl acetate, polyvinyl-pyrolidone) salts of acrylic acid polymers cellulose ethers and natural gums. Polymeric stabilizers used in inverse suspension polymerization reactions include block copolymers poly (hydroxy-stearic acid) co-poly ethylene oxide. Surfactants used for oil in water suspensions include spans and the anionic emulsifier.

2.8 Conducting Polymers

Alan MacDiarmid, Hideki Shirakawa and their research groups discovered conducting polymers and the ability to dope these polymers over the full range from insulator to metal. This particularly exciting because it created a new field of research on the boundary between chemistry and condensed matter physics. Conducting polymers offered the promise of achieving a new generation of polymers materials that exhibit the electrical and optical properties of metals or semiconductors and that retain the attractive mechanical properties and processing advantages of polymers [16].

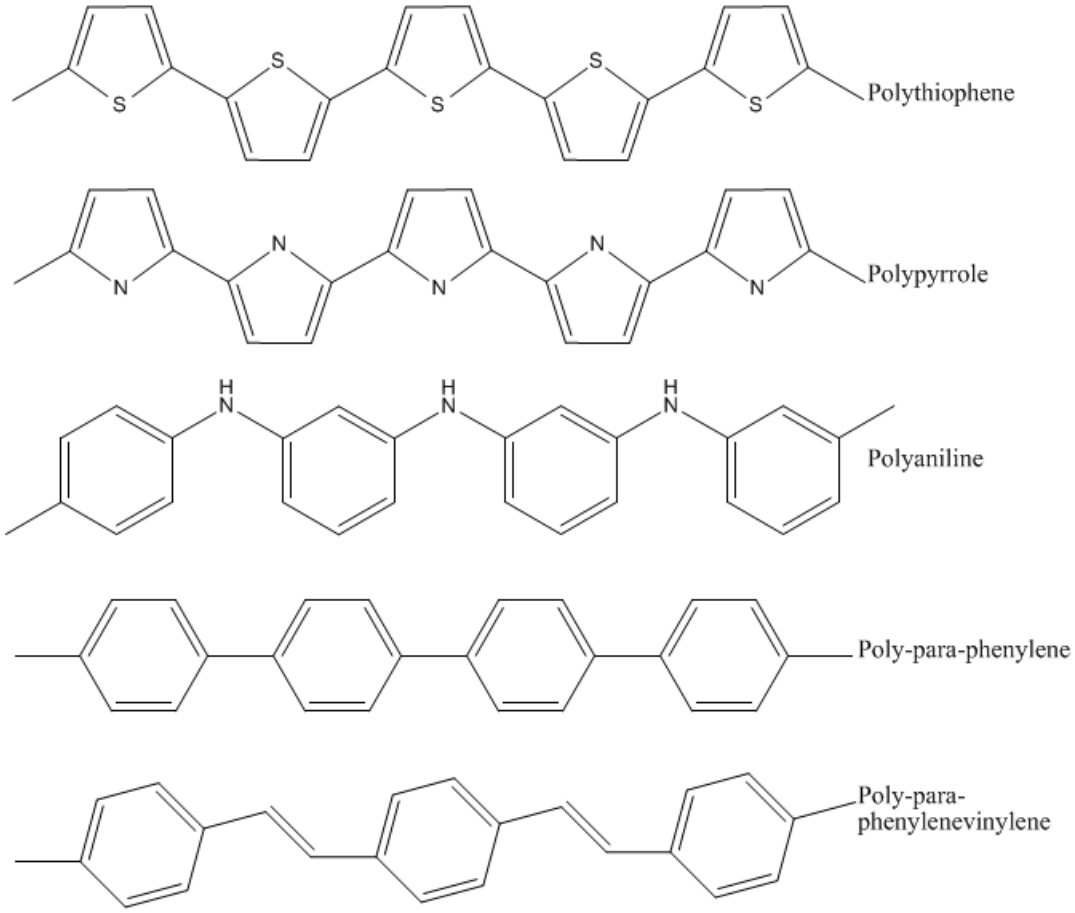

Figure 2.3: Molecular structure of typical conducting polymers

For electrical conductivity to occur on an electron must have a vacant place to move and occupy. When bands are completely filled or empty conduction can not occur . Metals are highly conductive because they possess unfilled bands. Semiconductors possess an energy gap small enough that thermal excitation of electrons from the valance to the conduction bands is sufficient for conductivity however the band gap in insulators is too large for thermal excition of electron across the band gap [17].

2.8.1 Band gap

A band gap, also called an energy gap or band-gap, is an energy range in a solid where no electron states exist. In a graph of the electronic band structure of a solid, the band gap generally refers to the energy difference (in electron volts) between the top of the valence band and the bottom of the conduction band which is found in insulators and semiconductors. It is the amount of energy required to free an outer shell electron from its orbit about the nucleus to become a mobile charge carrier, able

to move freely within the solid material. In conductors, the two bands often overlap, so they may not have a band gap.

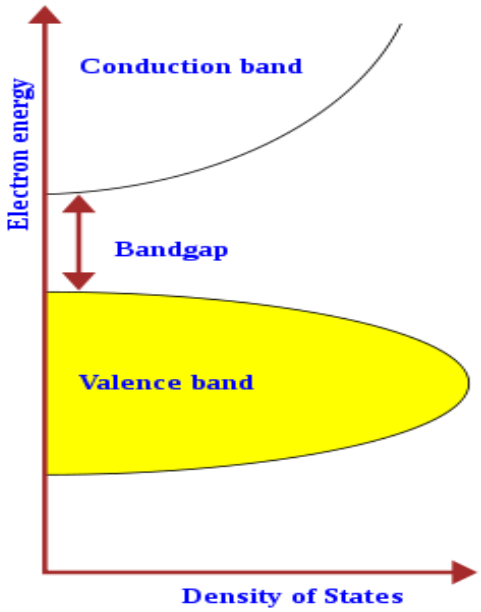

Figure 2.4: Semiconductor band structure.

In semiconductors and insulators, electrons are confined to a number of bands of energy, and forbidden from other regions. The term "band gap" as shown figure 2.4. refers to the energy difference between the top of the valence band and the bottom of the conduction band; electrons are able to jump from one band to another. In order for an electron to jump from a valence band to a conduction band, it requires a specific minimum amount of energy for the transition. The required energy differs with different materials. Electrons can gain enough energy to jump to the conduction band by absorbing either a phonon (heat) or a photon (light).

A material with a small but non-zero band gap which behaves as an insulator at absolute zero but allows thermal excitation of electrons into its conduction band at temperatures which are below its melting point is referred to as a semiconductor. A material with a large band gap is called an insulator. In conductors, the valence and conduction bands may overlap, so they may not have a band gap. The distinction between semiconductors and insulators is a matter of convention. One approach is to think of semiconductors as a type of insulator with a narrow band gap. Insulators with a larger band gap, usually greater than 3 eV, are not considered semiconductors

and generally do not exhibit semiconductive behaviour under practical conditions [18].

2.9 Semiconductor Basics

Expecting that the introduction of p-conjugated crosslinks between the conjugated macromolecules could represent an approach for the design of (semi)conducting polymers with increased charge-transport characteristics embarked on the exploration of conjugated polymer networks. In the use of poly(p-phenylene-ethylnylene) (PPE) derivatives it was demonstrated that that such networks may exhibit substantially better charge-transport characteristic than their linear parent polymers. These materials can, at least in part, overcome the problems associated with limited inter chain charge transfer between individual macromolecules. The concept of cross-linked networks has been extended by others to polythiophenes, mainly with the objective of improving the charge-carrier mobility or conductivity in undoped systems. Indeed, it was shown in both systems that small fractions of cross-linkers can increase the charge-carrier mobility or conductivity by more than an order of magnitude [19].

Semiconductors get their name from conduct electricity better than an insulator but not as well as a conductor. This arises from the nature of the bonds between atoms and their electrons in the solid. The difference can be explained by considering electrons to be in one of two levels: a *valence band* in which they are bound to atoms, and a *conduction band* in which they are free to move around in the solid. The valence band is at a higher energy level than the conduction band, but in a conductor the top of the valence band overlaps with the bottom of the conduction band, as shown in Figure 2.5. This reflects the low-energy bonding of electrons to metal atoms, which allows electrons to move and carry current easily in conductors. [20].

Silicon is used to create most inorganic semiconductors commercially, other materials are used, including germanium, gallium arsenide, and silicon carbide. A pure semiconductor is often called an “intrinsic” semiconductor.

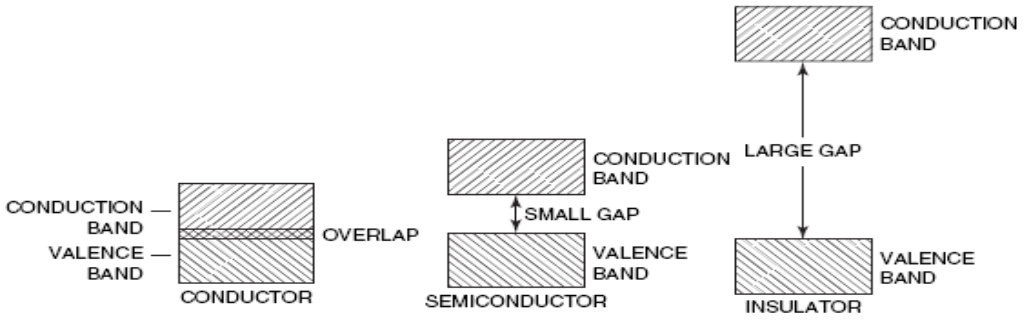

Figure 2.5: Bandgap comparison of insulators, semiconductors and metals

In an insulator, the band gap is large, so a valence electron needs so much energy to escape that essentially no electrons are free to conduct current .

The conductivity, or ability to conduct, of common semiconductor materials can be drastically changed by adding other elements, called "impurities" to the melted intrinsic material and then allowing the melt to solidify into a new and different crystal. This process is called "doping".

The number of electrons N in the valence and conduction bands depends on the bandgap energy ΔE and the temperature T:

$$\frac{N_{conduction}}{N_{valence}} = \exp^{\frac{\Delta E}{kT}} \quad \textbf{(2.1)}$$

where k is the Boltzmann constant. This is the same formula used to describe the relative proportions of atoms and molecules in a pair of different energy levels [21].

2.9.1 Doping and dopants

The property of semiconductors that makes them most useful for constructing electronic devices is that their conductivity may easily be modified by introducing impurities into their crystal lattice. The process of adding controlled impurities to a semiconductor is known as doping. The amount of impurity, or dopant, added to an intrinsic (pure) semiconductor varies its level of conductivity. Doped semiconductors are often referred to as extrinsic. By adding impurity to pure semiconductors, the electrical conductivity may be varied not only by the number of impurity atoms but also, by the type of impurity atom and the changes may be thousand folds and million folds [22].

The materials chosen as suitable dopants depend on the atomic properties of both the dopant and the material to be doped. In general, dopants that produce the desired

controlled changes are classified as either electron acceptors or donors. A donor atom that activates (that is, becomes incorporated into the crystal lattice) donates weakly-bound valence electrons to the material, creating excess negative charge carriers. These weakly-bound electrons can move about in the crystal lattice relatively freely and can facilitate conduction in the presence of an electric field. (The donor atoms introduce some states under, but very close to the conduction band edge. Electrons at these states can be easily excited to the conduction band, becoming free electrons, at room temperature). Conversely, an activated acceptor produces a hole. Semiconductors doped with donor impurities are called n-type, while those doped with acceptor impurities are known as p-type. The n and p type designations indicate which charge carrier acts as the material's majority carrier. The opposite carrier is called the minority carrier, which exists due to thermal excitation at a much lower concentration compared to the majority carrier [23].

2.9.2 Polaron theory

L. D. Landau and S. I. Pekar formed the basis of polaron theory. A charge placed in a polarizable medium can be screened. Dielectric theory describes the phenomenon by the induction of a polarization around the charge carrier. The induced polarization will follow the charge carrier when it is moving through the medium. The carrier together with the induced polarization is considered as one entity, which schematically shown in Figure 2.6.

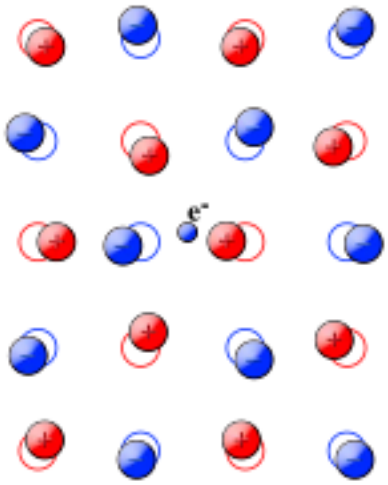

Figure 2.6: A view of a polaron

A conduction electron in an ionic crystal or a polar semiconductor repels the negative ions and attracts the positive ions. A self-induced potential arises, which acts back on the electron and modifies its physical properties as seen in figure 2.6.

The resulting lattice polarization acts as a potential well that hinders the movements of the charge, thus decreasing its mobility. Polarons have spin, though two close-by polarons are spinless. The latter is called a bipolaron. A conduction electron in an ionic crystal or a polar semiconductor is the prototype of a polaron.

An organic semiconductor is an organic material with semiconductor properties. Single molecules, short chain (oligomers) and organic polymers can be semiconductive. Semiconducting small molecules (aromatic hydrocarbons) include the polycyclic aromatic compounds pentacene, anthracene, and rubrene. Polymeric organic semiconductors include poly(3-hexylthiophene), poly(p-phenylene vinylene), as well as polyacetylene and its derivatives.

There are two major overlapping classes of organic semiconductors. These are organic charge-transfer complexes and various linear-backbone conductive polymers derived from polyacetylene. Linear backbone organic semiconductors include polyacetylene itself and its derivatives polypyrrole, and polyaniline. At least locally, charge-transfer complexes often exhibit similar conduction mechanisms to inorganic semiconductors. Such mechanisms arise from the presence of hole and electron conduction layers separated by a band gap. While such classic mechanisms are important locally, as with inorganic amorphous semiconductors, tunnelling, localized states, mobility gaps, and phonon-assisted hopping also significantly contribute to conduction, particularly in polyacetylenes. Like inorganic semiconductors, organic semiconductors can be doped. Organic semiconductors susceptible to doping such as polyaniline (Ormecon) and PEDOT:PSS are also known as organic metals.

Typical current carriers in organic semiconductors are holes and electrons in π-bonds. Almost all organic solids are insulators. But when their constituent molecules have π-conjugate systems, electrons can move via π-electron cloud overlaps, especially by hopping, tunnelling and related mechanisms. Polycyclic aromatic hydrocarbons and phthalocyanine salt crystals are examples of this type of organic semiconductor.

Mainly due to low mobility, even unpaired electrons may be stable in charge-transfer complexes. Such unpaired electrons can function as current carriers. This type of semiconductor is also obtained by pairing an electron donor molecule with an electron acceptor molecule.

2.10 Composites

A composite is a structural material that consists of two or more combined constituents that are combined at a macroscopic level. One constituent is called the reinforcing phase and the one in which it is embedded is called the matrix. The reinforcing phase material may be in the form of fibers, particles, or flakes. The matrix phase materials are generally continuous. Examples of composite systems include concrete reinforced with steel and epoxy reinforced with graphite fibers, etc. If the composite is designed and fabricated correctly, it combines the strength of the reinforcement with the toughness of the matrix to achieve a combination of desirable properties not available in any single conventional material [24].

2.10.1 Polymer matrix composite

The most common advanced composites are polymer matrix composites (PMCs) consisting of a polymer (e.g., epoxy, polyester, urethane) reinforced by thin diameter fibers (e.g., graphite, aramids, boron), metals, ceramics and so on. For example, graphite/epoxy composites are approximately five times stronger than steel on a weight-for-weight basis. The reasons why they are the most common composites include their low cost, high strength, and simple manufacturing principles [25]. They are designed and manufactured for various applications including automotive components, sporting goods, aerospace parts, consumer goods, and in the marine and oil industries.

The matrix material used in polymer-based composites can either be thermoset (epoxies, phenolics) or thermoplastic resins (low density polyethylene, high density polyethylene, polypropylene, nylon, acrylics). The filler or reinforcing agent can be choosen according to the desired properties. The properties of polymer matrix composites are determined by properties, orientation and concentration of fibers and properties of matrix.

2.10.2 Nanocomposites

Nanocomposites are a special class of materials originating from suitable combinations of two or more such nanoparticles or nanosized objects in some suitable technique, resulting in materials having unique physical properties and wide application potential in diverse areas.

2.11 Polypyrrole

Polypyrrole (PPy) is used for commercial applications because of its good environmental stability, facile synthesis, and higher conductivity than many other conducting polymers. PPy can often be used as biosensors, gas sensors, wires, microactuators, antielectrostatic coatings, solid electrolytic capacitor, electrochromic windows and displays, and packaging, polymeric batteries, electronic devices and functional membranes, etc. PPy can be easily prepared by either an oxidatively chemical or electrochemical polymerization of pyrrole. However synthetically conductive PPy is insoluble and infusible, which restricts its processing and applications in other fields. The problem has been extensively investigated and new application fields have also been explored in the past several years. For example, PPy-based polymers can be used to load and release drugs and biomolecules. PPy-based polymer blends can protect the corrosion of metals. Because of the strong adhesion of PPy to iron or steel treated with nitric acid, PPy polymers can be used as good adhesives.

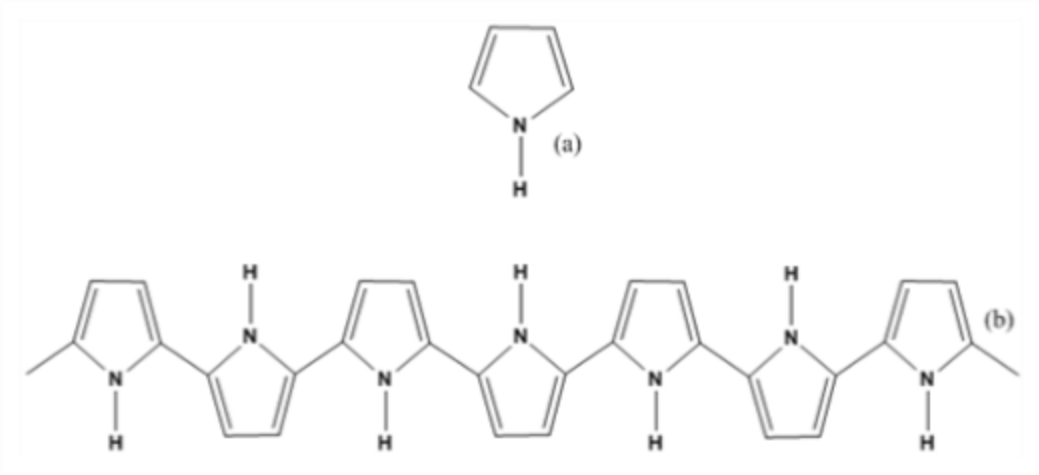

Figure 2.7: Chemical structure of (a) pyrrole and (b) polypyrrole

2.11.1 Synthesis of polypyrrole

Among other conducting polymers, PPy and its derivatives are of particular interest, owing to their high conductivity, stability in the oxidised state and interesting redox properties. The simplicity of the synthetic procedures and availability of the initial monomers are also attractive features of PPy. Chemical synthesis of PPy can be realized by oxidation of the monomer with chemical oxidants has a form of black powder. Aqueous or anhydrous $FeCl_3$, other salts of iron(III) and copper(II) are widely used as chemical oxidants. The use of halogens and organic electron acceptors as oxidants for PPy synthesis has also been reported. The yield and conductivity of the PPy produced are affected by a variety of factors, among which are the choice of solvent and oxidant, initial pyrrole/oxidant ratio, duration and temperature of the reaction. At the optimal ratio of Fe(III)/monomer which is 2.4, the yield of PPy approaches 100%. Shorter times of polymerisation and lower temperatures (0 to 5 ^oC) result in enhanced conductivity of PPy produced. For PPy prepared by monomer oxidation with $FeCl_3$ in various solvents (water, alcohols, benzene, tetrahydrofuran, chloroform, acetone, acetonitrile, dimethylformamide), the highest conductivity was observed for PPy prepared in methanol solution (190 Scm^{-1}). Controlled variation of the oxidising potential of the reaction medium [it was changed through the ratio of $FeCl_3$ to $FeCl_2$ and also using a binary acetonitrile/methanol solvent], provided a possibility to enhance conductivity of PPy to 220 Scm^{-1} in the former case and to 328 S cm^{-1} in the latter. When PPy is produced by oxidation in the presence of $FeCl_3$, the polymer is doped with Cl- anions; the overall reaction can be represented by the following stoichiometric equation where y is the degree of PPy oxidation (doping level).

$$nC_4H_5N + (2+y)nFeCl_3 = [(C_4H_3N)ny+ nyCl^-] + (2+y)nFeCl_2 + 2n\ HCl\ (...)$$

In earlier works, the degree of PPy oxidation was determined from the Cl/N ratio using the data from elemental analysis. The Cl/N ratio varied from 0.21 to 0.34. The Cl/N ratio for PPy prepared from aqueous solution was 0.33 and substantially exceeded that for the polymer produced from methanol and AN. X-Ray photoelectron spectroscopy (XPS) revealed that chlorine atoms in the polymer are in three chemical states, namely, ionic, covalently bonded and an intermediate one; the latter is similar to the chloride anions in metal chlorides (including $FeCl_3$ and $FeCl_2$). It was noticed that when PPy was treated with solution of $FeCl_3$ in nitromethane, the

iron-containing $FeCl_4^-$ anions were incorporated in the polymer. Possibly, the intermediate species of chlorine is related to iron chlorides. In spite of the high concentration of incorporated chlorine, only a Cl/N ratio equal to 0.25 corresponded to y (25% of oxidised monomer units). Thus, the elemental analysis is insufficient to determine the true degree of PPy oxidation.

The conductivity and stability of PPy powder produced by means of chemical oxidation were substantially improved. However, formation of PPy films or coatings on another material remained problematic. This problem was partially solved by PPy deposition from gas with $FeCl_3$ used as an oxidant. This method provided a possibility of producing free film or PPy coatings having high mechanical properties on substrates of any shape [26].

Electrochemical polymerisation provides a number of advantages over chemical methods. The first is that the reaction product is an electroactive film attached to the electrode surface and having high conductivity. Second is that the yield in charge terms is close to 100%; this provides a possibility of controlling the mass and thickness of the film. And finally, the properties of the film produced can be controlled directly in the course of preparation. In electrochemical oxidation method, pyrrole and an electrolyte salt are dissolved in a suitable solvent and then the solution is subjected to oxidation, resulting in the growth of a conducting PPy film on the anodic working electrode.

Electropolymerisation of pyrrole can be performed in both aqueous and non-aqueous media, such as AN, propylene carbonate (PC), dichloromethane. However, with increasing nucleophilicity of solvent, the film growth is inhibited due to the interaction of solvent with the primary products of monomer oxidation. The film does not form in such nucleophilic aprotic solvents as dimethylformamide, dimethyl sulfoxide, hexamethylphosphoramide, unless the nucleophilicity of solvent is reduced by addition of a protic acid. Apart from that, the side reactions occurring on the film surface can affect electropolymerisation in these solvents. Thus, a thick PPy film was prepared from a $NaClO_4$ solution in dimethylformamide. An increase in the rate of electropolymerisation was observed when the temperature decreased. This increase was explained by the relative inhibition of the side reaction of film passivation, which resulted in lower conductivity. The rate of electropolymerisation

grew with increasing concentration of ClO_4^- anions that act as retardants for the passivating reactions in the electrolyte [27].

2.12 Electrospinning and Nanofibers

Conventional fiber spinning (like melt, dry and wet spinning) produce fibers with diameter in the range of micrometer. In recent years, electrospinning has gained much attention as a useful method to prepare fibers in nanometer diameter range. These ultra-fine fibers are classified as nanofibers. The unique combination of high specific surface area, extremely small pore size, flexibility ad superior directional strength makes nanofibers a preferred material form for many applications. Proposed uses of nanofibers include wound dressing, drug delivery, tissue scaffolds, protective clothing, filtration, reinforcement and micro-electronics

2.12.1 Fundamental aspect

There are basically three components to fulfill the process: a high voltage supplier, a capillary tube(syringe) with a pipette or needle of small diameter, and a metal collecting screen. In the electrospinning process a high voltage is used to create an electrically charged jet of polymer solution or melt out of the pipette. Before reaching the collecting screen, the solution jet evaporates or solidifies, and is collected as an interconnected web of small fibers [28,29]. One electrode is placed into the spinning solution/melt and the other attached to the collector. In most cases, the collector is simply grounded, The electric field is subjected to the end of the capillary tube that contains the solution fluid held by its surface tension. This induces a charge on the surface of the liquid. Mutual charge repulsion and the contraction of the surface charges to the counter electrode cause a force directly opposite to the surface tension [30]. Meanwhile, the solvent evaporates, leaving behind a charged polymer fiber. In the case of the melt the discharged jet solidifies when it travels in the air. The process does not require the use of coagulation chemistry or high temperatures to produce solid threads from solution. This makes the process particularly suited to the production of fibers using large and complex molecules. Electrospinning from molten precursors is also practised; this method ensures that no solvent can be carried over into the final product.

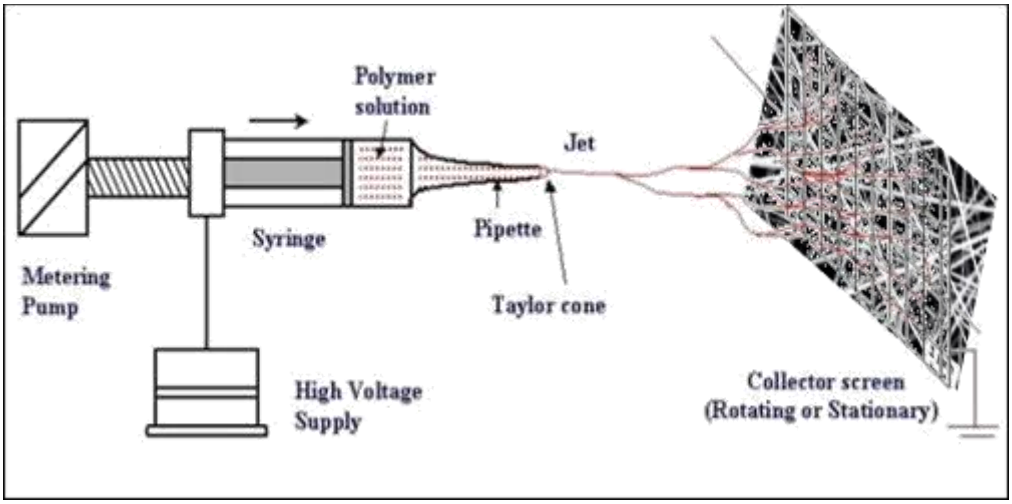

Figure 2.8: Typical setup of electrospinning device

2.12.2 Effects on electrospinning of fibers

Many parameters can influence the transformation of polymer solutions into nanofibers through electrospinning. These parameters include (a) the solution properties such as viscosity, elasticity, conductivity, and surface tension, (b) governing variables such as hydrostatic pressure in the capillary tube, electric potential at the capillary tip, and the gap (distance between the tip and the collecting screen), and (c) ambient parameters such as solution temperature, humidity, and air velocity in the electrospinning chamber [31].

One of the most important quantities related with electrospinning is the fiber diameter. Since nanofibers are resulted from evaporation or solidification of polymer fluid jets, the fiber diameters will depend primarily on the jet sizes as well as on the polymer contents in the jets.

2.12.3 Solution properties

As long as no splitting is involved, one of the most significant parameters influencing the fiber diameter is the solution viscosity. A higher viscosity results in a larger fiber diameter [32]. However, when a solid polymer is dissolved in a solvent, the solution viscosity is proportional to the polymer concentration. Thus, the higher the polymer concentration the larger the resulting nanofiber diameters will be.

There are several factors affecting solution viscosity. Molecular weight, polymer chain entanglement, concentration, and temperature are accepted as the main factors. Molecular weight of a polymer is directly related to viscosity of the solution.

Generally, when a polymer of higher molecular weight is dissolved in a solvent, its viscosity will be higher than solution of the same polymer but of a lower molecular weight. One of the conditions necessary for electrospinning to occur where fibers are formed is that the solution must consists of polymer of sufficient molecular weight and the solution must be of sufficient viscosity. As the jet leaves the needle tip during electrospinning, the polymer solution is stretched as it travels towards the collection plate. During the stretching of the polymer solution, it is the entanglement of the molecule chains that prevents the electrically driven jet from breaking up thus maintaining a continuous solution jet. As a result, monomeric polymer solution does not form fibers when electrospun [33].

Solution Viscosity

The viscosity measured in a capillary viscometer is not obtained at a defined shear rate. Of several fixes to this problem, the simplest is simply to ignore it. This amounts to assuming that the fluid is Newtonian over the entire range of shear rates encountered by the fluid as it passes down the capillary.

The Ubbelohde capillary viscometer

The most useful kind of viscometer for determining intrinsic viscosity is the suspended level or Ubbelohde viscometer, the viscometer is called suspended level because the liquid initially drawn into the small upper bulb is not connected to the reservoir as it flows down the capillary during measurement. The capillary is suspended above the reservoir. In conjunction with the pressure-equalization tube, this ensures that the only pressure difference between the top of the bulb and the bottom of the capillary is that due to the hydrostatic pressure the weight of the liquid. Such viscometers are useful in other experiments checking the stability of some polymer solution, where one is only interested in measuring a change in the flow time.

Use of the Ubbelohde viscometer

Capillary viscometry is conceptually simple: the time it takes a volume of polymer solution to flow through a thin capillary is compared to the time for a solvent flow. It turns out that the flow time for either is proportional to the viscosity, and inversely proportional to the density.

$$t_{solvent} = \frac{\eta_{solvent}}{\rho_{solvent}} \quad \textbf{(2.2)}$$

$$t_{sol'n} = \frac{\eta_{sol'n}}{\rho_{sol'n}} \quad \textbf{(2.3)}$$

relative viscosity to be the ratio $\eta_{sol'n} / \eta_{solvent}$. For most polymer solutions at the concentrations of interest, $\rho_{sol'n} / \rho_{solvent} \approx 1$. Thus, to a very good approximation, the relative viscosity is a simple time ratio:

$$\eta_{rel} = t_{sol'n} / t_{solvent} \qquad \textbf{(2.4)}$$

specific viscosity to be the fractional change in viscosity upon addition of polymer:

$$\eta_{sp} = \frac{\eta_{sol'n} - \eta_{solvent}}{\eta_{solvent}} \text{ (Unitless)} \qquad \textbf{(2.5)}$$

Both η_{rel} and η_{sp} depend on the polymer concentration, so to extract the "intrinsic" properties of the polymer chain itself, one must extrapolate to zero concentration. Measuring *at* zero concentration (c=0) would be useless, but this concept of extrapolating *to* c=0 is very important in polymer characterization and in thermodynamics generally. The two quantities that are commonly plotted *vs.* concentration and extrapolated to c=0 are η_{sp} and $c^{-1} ln(\eta_{rel})$.

both plots have the same intercept, which is called $[\eta]$, the intrinsic viscosity.

$$[\eta] = \lim_{c \to 0} \frac{\eta_{sp}}{c} \equiv \lim_{c \to 0} c^{-1} \ln \eta_{rel} \qquad \textbf{(2.6)}$$

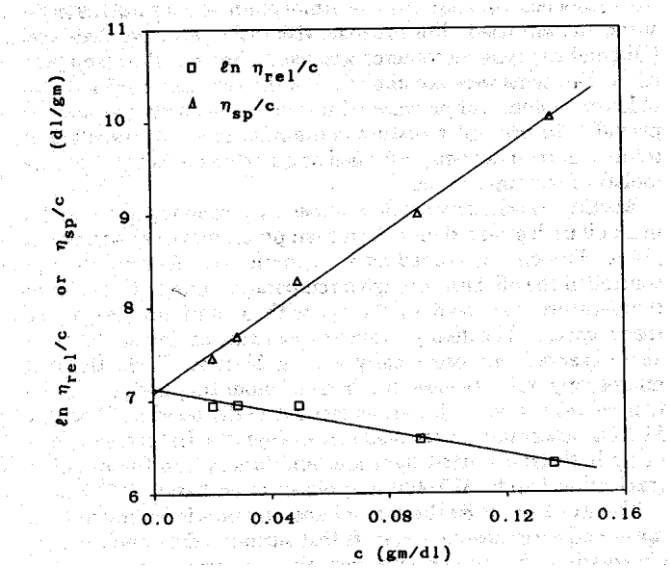

where M is the polymer molecular weight. Thus, $[\eta]^{-1}$ is approximately the concentration within the polymer, or the "overlap concentration". At concentrations exceeding about $[\eta]^{-1}$ polymer molecules will touch and interpenetrate. The "semidilute" regime of polymers begins here. More importantly for our purposes is the scaling relationship between $[\eta]$ and molecular weight:

$$[\eta] = KM^{a} \quad \text{(Mark-Houwink Relationship)} \qquad \textbf{(2.7)}$$

Thus, log-log plots of $[\eta]$ against molecular weight have the intercept log(K) and slope a. The slope contains information about the shape of the molecules:
A more modern way to generate Mark-Houwink plots is to couple a GPC apparatus to an on-line intrinsic viscometer. Ideally, one uses *three* detectors (concentration detector, light scattering detector and intrinsic viscosity detector). The first two determine molecular weight absolutely, while the third provides $[\eta]$.

$a = 1/2 \Rightarrow$ flexible polymer chain in "ideal" solvent

$0.5 < a < 0.8 \Rightarrow$ flexible polymer chain in "good" solvent (excluded volume limit)

$a > 0.8 \Rightarrow$ "stiff" chain

A given chain in any good solvent will have the same $[\eta]$. In that sense, $[\eta]$ really is a property *intrinsic* to the chain--but only inasmuch as the polymer conformation is partly determined by the solvent [34].

2.12.4 Molecular weigth

The molecular weight of the polymer represents the length of the polymer chain, which in turn have an effect on the viscosity of the solution since the polymer length will determine the amount of entanglement of the polymer chains in the solvent. Another way to increase the viscosity of the solution is to increase the polymer concentration . Increasing solution concentration shows almost same effect as using higher molecular weight polymer. Polymer chain entanglement of the polymer solution is improved in either case. At higher concentrations, viscosity of the solution becomes higher and it prevents the jet having larger bending instabilities. This causes small deposition on the collecting media for fibers and the resultant fiber diameter is thickened. At low viscosities, there will be less amount of chain entanglement in polymer solution. The forces from surface tension become dominant and bead formation occurs along the string of electrospun fibers. At high viscosities, jets can be stretched fully and beadless fibers can be obtained. High viscosity values also

provoke splitting of jets into smaller fibers. Moreover, pumping of the polymer solution becomes difficult and drying of the solution on the tip of the pipette can be observed [35, 36].

2.12.5 Surface tension

The initiation of electrospinning requires the charged solution to overcome its surface tension. However, as the jet travels towards the collection plate, the surface tension may cause the formation of beads along the jet . Surface tension has the effect of decreasing the surface area per unit mass of a fluid. In this case, when there is a high concentration of free solvent molecules, there is a greater tendency for the solvent molecules to congregate and adopt a spherical shape due to surface tension. A higher viscosity will means that there is greater interaction between the solvent and polymer molecules thus when the solution is stretched under the influence of the charges, the solvent molecules will tend to spread over the entangled polymer molecules thus reducing the tendency for the solvent molecules to come together [37, 38, 39].

2.12.6 Solution conductivity

Electrospinning involves stretching of the solution caused by repulsion of the charges at its surface. Thus if the conductivity of the solution is increased, more charges can be carried by the electrospinning jet. As a result, smooth fibers are formed which may otherwise yield beaded fibers. The increased in the stretching of the solution also will tend to yield fibers of smaller diameter . However, there is a limit to the reduction in the fiber diameter. Solution prepared using solvents of higher conductivity generally yield fibers without beads while no fibers are formed if the solution has zero conductivity.

2.12.7 Dielectric effect of solvent

The dielectric constant of a solvent has a significant influence on electrospinning. Generally, a solution with a greater dielectric property reduces the beads formation and the diameter of the resultant electrospun. Solvents such as N,N-Dimethylformamide (DMF) may added to a solution to increase its dielectric property to improve the fiber morphology. The bending instability of the electrospinning jet also increases with higher dielectric constant. This is shown by

increased deposition area of the fibers. However, if a solvent of a higher dielectric constant is added to a solution to improve the electrospinnability of the solution, the interaction between the mixtures such as the solubility of the polymer will also have an impact on the morphology of the resultant fibers. Dielectric constants of solvents are another important parameter for the finak fiber properties as shown in Table 2.1.

Table 2.1: Dielectric constants of solvents [40].

Solvent	**Dielectric constant**
Water	80.02
Acetonitrile	35.92-37.06
Dimethylformamide	36.71
Methanol	32.60
Trifluoroethanol	27.00
Ethanol	24.55
Acetone	20.7
2-propanol	18.3
Pyridine	12.30
m-Cresol	11.80
Dichloromethane	8.93
Tetrahydrofuran	7.47
Acetic acid	6.15
Ethyl acetate	6.00
Chloroform	4.80
Toluene	2.40

Further challenge with current electrospinning lies in the fact that the fiber diameters obtained are seldom uniform. Not many reports have been given towards resolving this problem. While electrospinning polyurethane nanofibers, they recognized that the fiber diameters obtained from the polymer solution at a high (70 °C) temperature were much more uniform than those at room temperature.

2.12.8 Processing conditions

Another important parameter that affects the electrospinning process is the various external factors exerting on the electrospinning jet. This includes the voltage supplied, the feedrate, temperature of the solution, type of collector, diameter of needle and distance between the needle tip and collector. These parameters have a certain influence in the fiber morphology although they are less significant than the solution parameters.

2.12.8.1 Voltage

A crucial element in electrospinning is the application of a high voltage to the solution. The high voltage will induce the necessary charges on the solution and together with the external electric field, will initiate the electrospinning process when the electrostatic force in the solution overcomes the surface tension of the solution. If the applied voltage is higher, the greater amount of charges will cause the jet to accelerate faster and more volume of solution will be drawn from the tip of the needle.

As both the voltage supplied and the resultant electric field have an influence in the stretching and the acceleration of the jet, they will have an influence on the morphology of the fibers obtained. In most cases, a higher voltage will lead to greater stretching of the solution due to the greater columbic forces in the jet as well as the stronger electric field.

These have the effect of reducing the diameter of the fibers and also encourage faster solvent evaporation to yield drier fibers. When a solution of lower viscosity is used, a higher voltage may favor the formation of secondary jets during electrospinning. This has the effect of reducing the fiber diameter. Another factor that may influence the diameter of the fiber is the flight time of the electrospinning jet. A longer flight time will allow more time for the fibers to stretch and elongates

before it is deposited on the collection plate. Thus, at a lower voltage, the reduced acceleration of the jet and the weaker electric field may increase the flight time of the electrospinning jet which may favor the formation of finer fibers.

At a higher voltage, it was found that there is a greater tendency for beads formation. The shape of the beads changes from spindle-like to spherical-like with increasing voltage. Increasing voltage will increased the beads density, which at an even higher voltage, the beads will join to form a thicker diameter fiber [41].

2.12.8.2 Feedrate

The feedrate will determine the amount of solution available for electrospinning. When the feedrate is increased, there is a corresponding increase in the fiber diameter or beads size. This is apparent as there is a greater volume of solution that is drawn away from the needle tip [42].

2.12.8.3 Temperature

The temperature of the solution has both the effect of increasing its evaporation rate and reducing the viscosity of the polymer solution. This may be due to the lower viscosity of the solution and greater solubility of the polymer in the solvent which allows more even stretching of the solution. However, in cases where biological substances such as enzymes and proteins are added to the solution for electrospinning, the use of high temperature may cause the substance to lose its functionality.

2.12.8.4 Effect of collector

There must be an electric field between the source and the collector for electrospinning to initiate. Thus in most electrospinning setup, the collector plate is made out of conductive material such as aluminum foil which is electrically grounded so that there is a stable potential difference between the source and the collector. In the case when a nonconducting material is used as a collector, charges on the electrospinning jet will quickly accumulates on the collector which will result in fewer fibers deposited . This is caused by the repulsive forces of the accumulated charges on the collector as more fibers are deposited. For a conducting collector, charges on the fibers are dissipated thus allowing more fibers to be attracted to the collector. The fibers are able to pack closely together as a result [43].

2.12.8.5 Diameter of pipette orifice / needle

The internal diameter of the needle or the pipette orifice has a certain effect on the electrospinning process. A smaller internal diameter was found to reduce the clogging as well as the amount of beads on the electrospun fibers. Decrease in the internal diameter of the orifice was also found to cause a reduction in the diameter of the electrospun fibers. When the size of the droplet at the tip of the orifice is decreased, such as in the case of a smaller internal diameter of the orifice, the surface tension of the droplet increases. As a result, the acceleration of the jet decreases and this allows more time for the solution to be stretched and elongated before it is collected.

2.12.8.6 Distance between tip and collector

The flight time as well as the electric field strength will affect the electrospinning process and the resultant fibers. Varying the distance between the tip and the collector will have a direct influence in both the flight time and the electric field strength. For independent fibers to form, the electrospinning jet must be allowed time for most of the solvents to be evaporated. When the distance between the tip and the collector is reduced, the jet will have a shorter distance to travel before it reaches the collector plate. Moreover, the electric field strength will also increase at the same time and this will increase the acceleration of the jet to the collector. As a result, there may not have enough time for the solvents to evaporate when it hits the collector.

Depending on the solution property, the effect of varying the distance may or may not have a significant effect on the fiber morphology. In some cases, changing the distance has no significant effect on the fiber diameter. However, beads were observed to form when distance was too low. The formation of beads may be the resultof increased field strength between the needle tip and the collector.

Decreasing the distance has the same effect as increasing the voltage supplied and this will cause an increased in the field strength. If the field strength is too high, the increased instability of the jet may encourage beads formation . However, if the distance is such that the field strength is at an optimal value, there is less beads formed as the electrostatic field provides sufficient stretching force to the jet. In other circumstances, increasing the distance results in a decrease in the average fiber

diameter. The longer distance means that there is a longer flight time for the solution to be stretched before it is deposited on the collector However, there are cases where at a longer distance, the fiber diameter increases. This is due to the decrease in the electrostatic field strength resulting in less stretching of the fibers. When the distance is too large, no fibers are deposited on the collector. Therefore, it seems that there is an optimal electrostatic field strength below which the stretching of the solution will decrease resulting in increased fiber diameters.

2.12.8.7 Ambient parameters

The effect of the electrospinning jet surrounding is one area which is still poorly investigated. Any interaction between the surrounding and the polymer solution may have an effect on the electrospun fiber morphology. High humidity for example was found to cause the formation of pores on the surface of the fibers. Since electrospinning is influenced by external electric field, any changes in the electrospinning environment will also affect the electrospinning process.

2.13 Application Areas:

Applications are in the field of filtration systems and medical prosthesis mainly grafts and vessels. Other applications which have been targeted include tissue template, electromagnetic shielding, composite delamination resistance, and liquid crystal device.

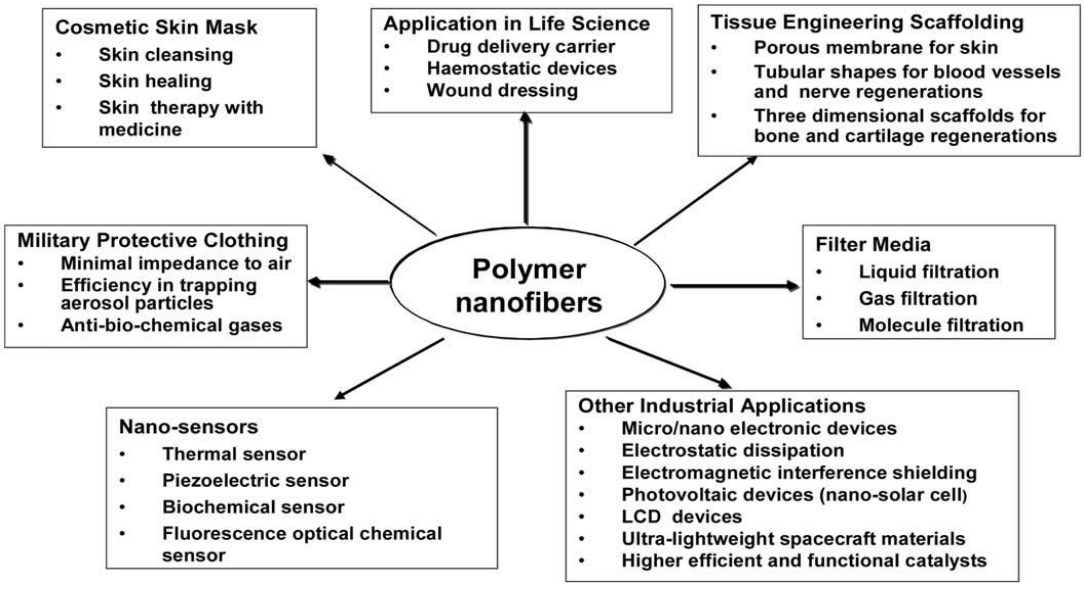

Figure 2.9: Application area of polymer nanofibers

The size of an electrospun fiber can be in the nano scale and the fibers may possess nano scale surface texture, leading to different modes of interaction with other materials compared with macroscale materials. In addition to this, the ultra-fine fibers produced by electrospinning are expected to have two main properties, a very high surface to volume ratio, and a relatively defect free structure at the molecular level. This first property makes electrospun material suitable for activities requiring a high degree of physical contact, such as providing sites for chemical reactions, or the capture of small sized particulate material by physical entanglement filtration. The second property should allow electrospun fibers to approach the theoretical maximum strength of the spun material, opening up the possibility of making high mechanical performance composite materials [44].

3. EXPERIMENTAL PART

3.1 Materials

Methyl Methacrylate (MMA, >99.5 %, Sigma Aldrich), n-Butyl Acrylate (BA, > 99.5%, Fluka), DMF (Dimethylformamide, C3H7NO, Riedel-de Haen, 90 % technical grade), (DMF), *Tetrahydrofuran (THF), Sodium Dodecyl Sulfate (SDS) and Potassium Peroxydisulfate* (KPS) were purchased from Sigma Aldrich. Acetone [$(CH_3)_2CO$, 90% technical grade] and Ethyl alcohol [(C2H5OH), 90% technical grade] were obtained from Merck. The pyrrole (Py) was Sigma Aldrich reagent. Ammonium Cerium (IV) nitrate $(NH_4)_2[Ce(NO_3)_6]$ (CAN, >98% titration) was Sigma Aldrich reagent. All these reagents were used as received.

3.2 Synthesis of P(BA-co-MMA)

0.5 g emulsifier sodium dodecyl sulfate was dissolved in 80 ml water and then 50 g of a mixture of monomers of MMA and BA (25:25 wt MMA:BA) were dropped into the reactor, the mixture was stirrred for 30 minutes. Monomers were shown in Figure 3.1. At the same time, 0.25 g KPS is dissolved in 20ml pure water. After the 30 minutes, dissolved KPS is added to the mixture. Monomer structures were shown in Figure 3.2.

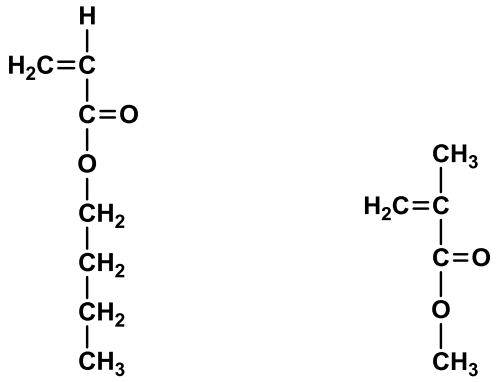

Figure 3.1: Monomers used in synthesis of P(BA-co-MMA), Butyl Acrylate (BA) and Methyl Methacrylate (MMA) respectively.

Reaction continued for 3 hours at 80 °C. Experimental setup of the polymerization was demonstrated in Figure 3.3. After the 3 hours, reaction was stopped with addition of 300 ml ethanol. Then the mixture was washed with ethanol and water and copolymer was dried at 50°C for 24 hour in vacuum drying-oven.

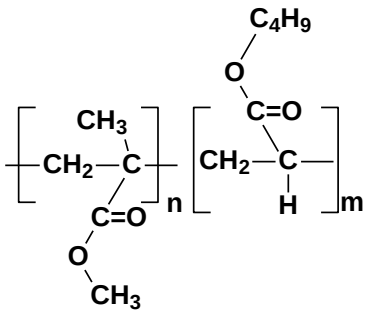

Figure 3.2: P(BA-co-MMA) structure.

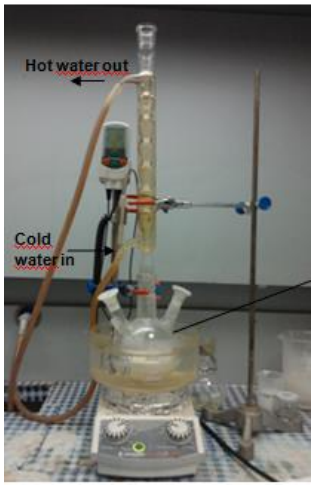

Figure 3.3:Experimental setup for synthesis of P(BA-co-MMA).

Table 3.1: BA and MMA composition in feed and copolymer

Copolymer	**Monomer Mole Fraction (mol %)[a]**		**Copolymer Mole Fraction (mol %)[b]**		**Yield[b] (%)**
	X_{BA}	X_{MMA}	X_{BA}	X_{MMA}	
P(BA-co-MMA)	50	50	17.85	82.1	60

[a]:Calculated gravimetrically

[b]:Determined from ^{1}H-NMR

X: fraction

3.3 Preparation of P(BA-co-MMA)/PPy Composites

Synthesized 0.5g P(BA-co-MMA) was dissolved in 10 ml dimethylformamide at room temperture and stirred for 3 hours. After pyrrole (i.e., 0.72, 1.44, 2.16, 2.88 mmoles) was introduced into the solution, mixture was stirred for 1 hour at 25°C. Cerium ammonium nitrate which is the 20% amount of pyrrole was dissolved in ACN. This solution was added P(BA-co-MMA) matrix drop by drop for the oxidation of pyrrole in P(BA-co-MMA) matrix . P(BA-co-MMA) / PPy solution was mixed for 12 hours. To terminate of reaction was 100 ml ethanol was added to matrix. The reaction is terminated. Polymer was washed by ethanol and pure water. Washed polymer was dried in the oven for 24 hours.

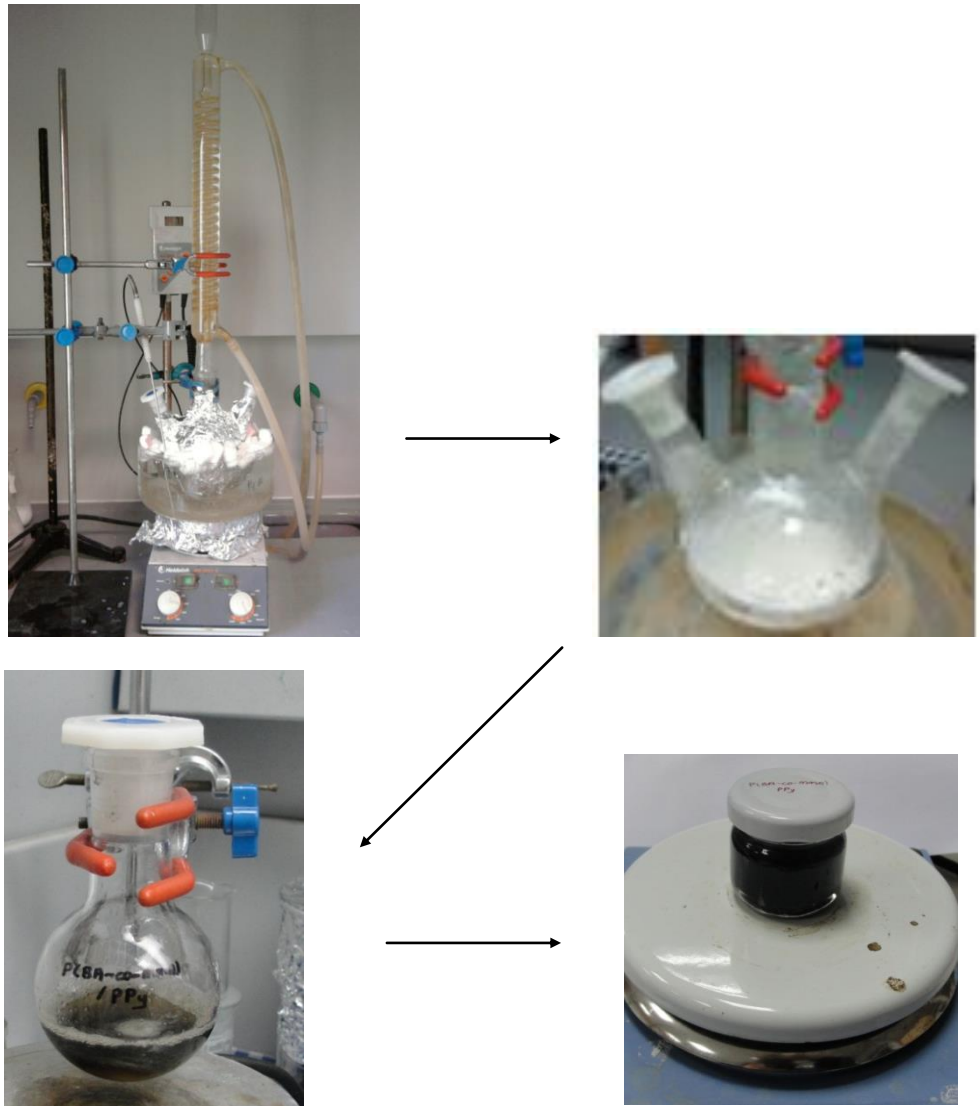

Figure 3.4: Polymerization of pyrrole in P(BA-co-MMA) composites

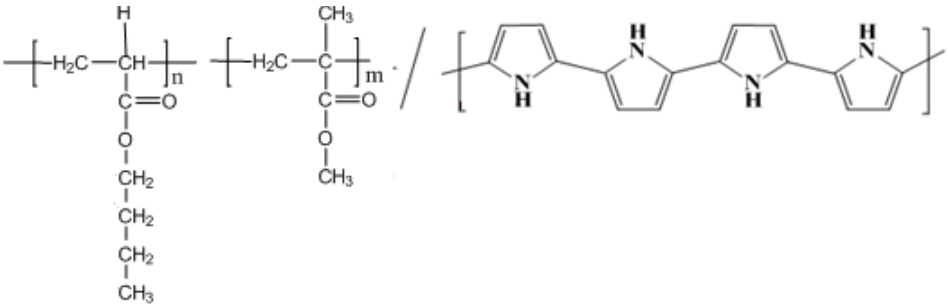

Figure 3.5: The structure of composite.

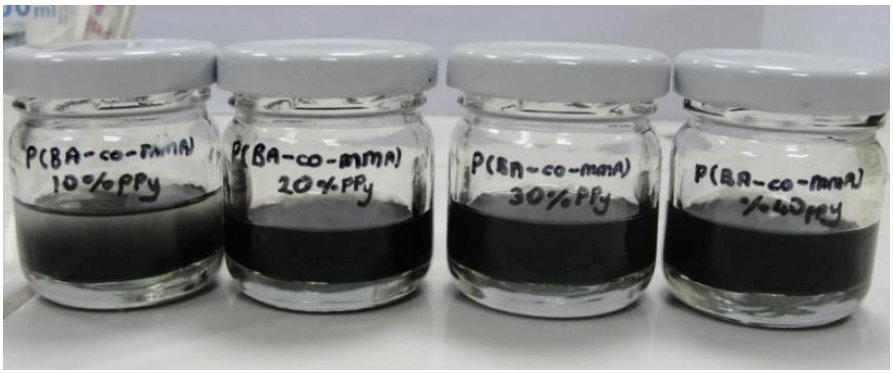

Figure 3.6: Composites with different polypyrrole composites

In this study, P(BA-co-MMA) has constant value as 5% wt conducting polymer as pyrrole amount is changed each study as shown in table 3.2.

Table 3.2: Feed content of Pyrrole

Sample of Composite	**Feed Pyrrole Amount (mmoles)**	**Feed Pyrrole Weight Fraction (%)**
P(BA-co-MMA)@PPy_1	0.72	10
P(BA-co-MMA)@PPy_2	1.44	20
P(BA-co-MMA)@PPy_3	2.16	30
P(BA-co-MMA)@PPy_4	2.88	40

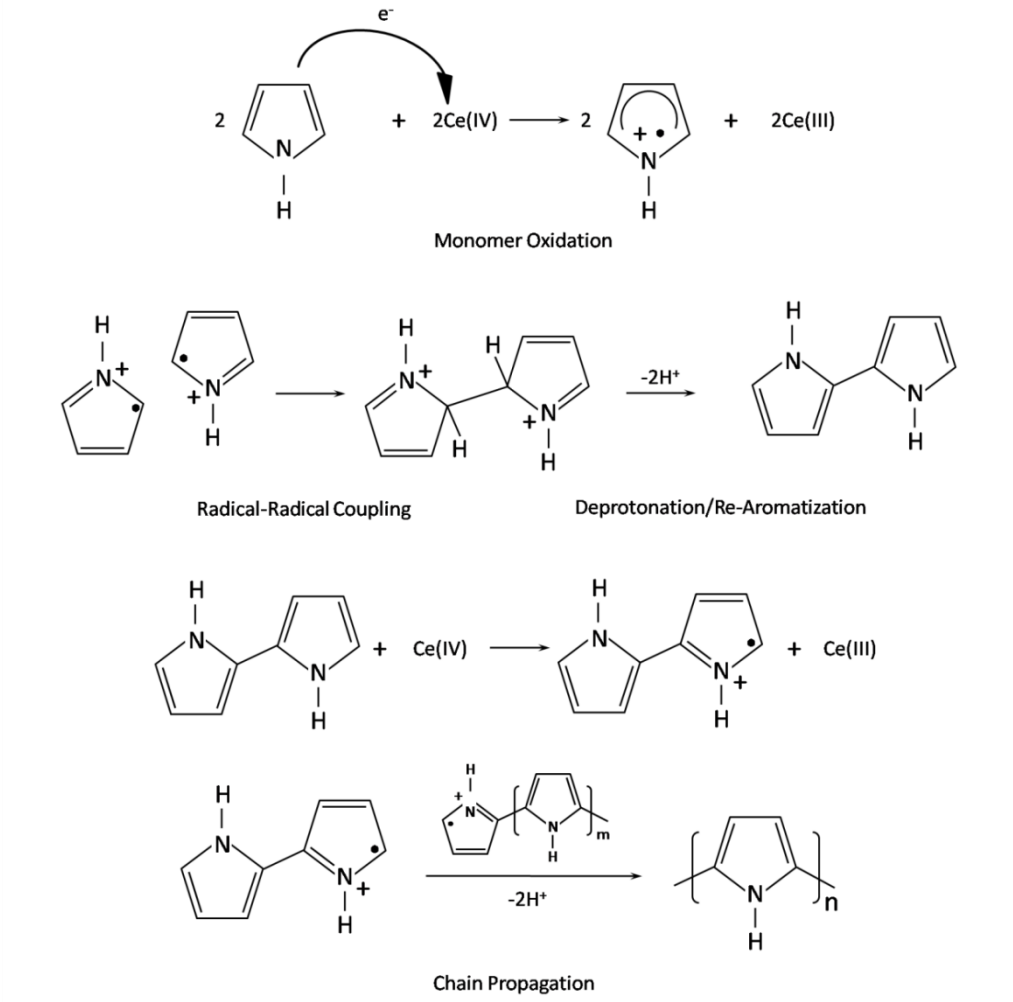

Figure 3.7: Polymerization mechanism of PPy

3.4 Preparation of P(BA-co-MMA) / PPy Composite Films

0.25 g P(BA-co-MMA) matrix was dissolved in 10 ml dimethylformamide , solvent casting of the viscous solution as a film on 5 x 5 cm^2 glass substrate area at about 1 mm height as seen in figure 3.8 . The casted solution were dried in an oven for one day at 760 mmHg and 50°C to evaporate the solvent as seen in figure 3.8 . The film thicknesses (≈ 80-130 μm) was measured with Mitutoyo Digimatic Outside Micrometer (MDC-25SB). Also each polypyrrole composites dissolved in same method. Each films have square shapes and nearly same thickness as seen figure 3.9. These films can be used for dynamic mechanical analyses equipment to measuring stress vs strength behaviour.

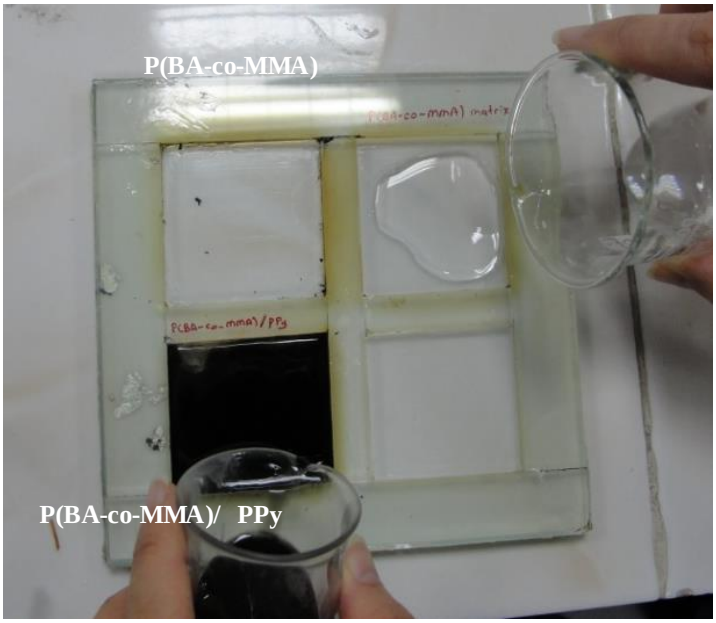

Figure 3.8: Viscous solution of composites on 5 x 5 cm^2 glass substrate

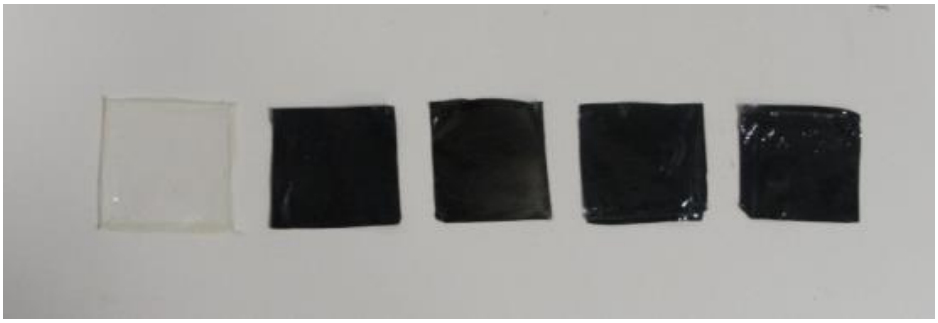

Figure 3.9: P(BA-co-MMA) and P(BA-co-MMA)/ PPy composite films

3.5 Preparation of Electrospinning Solutions

Four series of polymer solutions with different concentration of P(BA-co-MMA)/PPy were dissolved in DMF, THF and mixture of THF and DMF. For each solutions were stirred at room temperature with the speed of 300 rpm at 4 hour. The electrospinning apparatus consists of a syringe pump. The solutions were then loaded into a 2.5 ml syringe. Distance between tip and collector is 15 cm. The positive electrode wire was hooked at the metal part of the needle and negative part of the electrode was attached to the metal collector nearly 60 minutes of operation time was sufficient for the deposition of fibers on aluminum foil.

Table 3.3: Electrospinning parameters for various composites

Optimum Electrospinning Parameters	
Solution concentration	5 %
Applied voltage	15 kV
Tip-to-collector distance	15 cm
Feed rate	1.0 mL/h

3.6 Process Set up and Electrospinning

The positive electrode wire was hooked at the metal part of the needle and negative part of the electrode was attached to the Al metal collector 5 to 60 minutes of operation time was sufficient for the deposition of fibers on aluminum foil. A horizontal setup was chosen for electrospinning process. In electrospinning process, the setup consisted of a DC high voltage power supply from GAMMA High Voltage Research Inc., USA (Model no: ES50) with an electrical potential range from 0 to 30 kV, and a syringe pump (New Era Pump Systems Inc., USA Model no: NE-500). The metal collector was covered with an aluminum foil. The setup was kept in a plexiglass box for experimenter's safety. All experiments were carried out under atmospheric pressure and at room temperature

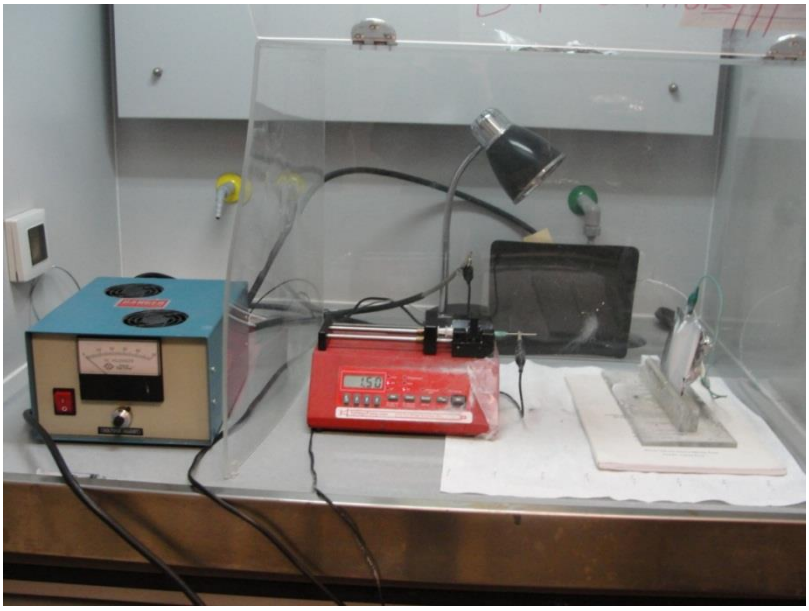

Figure 3.10: Experimental setup of electrospinning

3.7 Characterization of P(BA-co-MMA)/PPy composites

The structure of the copolymers was characterized by means of and Fourier Transform Infrared-Attenuated Total Reflectance (FTIR-ATR) spectroscopy, 1H NMR spectroscopy, by Ubbelodhe viscometer, Dynamic Mechanical Analyser, DMA, UV Visible Spectrophotometry, Contact Angle Meter, Novocontrol broadband dielectric spectrometer, Scanning Electron Microscope, GPC.

FTIR analysis of P(BA-co-MMA) and P(BA-co-MMA)@PPy_1, P(BA-co-MMA)@PPy_2, P(BA-co-MMA)@PPy_3, P(BA-co-MMA)@PPy_4 polymers in powder form and as nanofiber webs were carried out with FTIR-ATR reflectance spectrophotometer (Figure 3.11, Perkin Elmer, Spectrum One, with a Universal ATR attachment with a diamond and ZnSe crystal).

Figure 3.11: Perkin Elmer FTIR-ATR Spectrophotometer

^{1}H NMR spectroscopy by using 250 MHz Bruker AC Aspect 3000 NMR spectrometer and 500 MHz Agilent VNMRS Nuclear Magnetic Resonance Spectrometer (Figure) with deuterated chloroform, $CDCl_3$ as a solvent. Values were recorded as ppm relative to internal standard (TMS).

Figure 3.12: Agilent VNMRS 500 MHz Nuclear Magnetic Resonance Spectrometer

Viscosity average (Mv) molecular weight of P(BA-co-MMA) was determined in DMF solvent using Ubbelohde equipment. The intrinsic viscosity of the polymer solutions in DMF was determined by Ubbelodhe viscometer for P(BA-co-MMA).

Thermal and mechanical properties of molded films obtained by polymer composites were measured by using a TA Q800 Dynamic Mechanical Analyser, DMA (Figure 3.13). Thermal measurements of polymeric films were operated by multi- frequency-strain test method. Samples were heated from the ambient temperature to 150 °C by a heating rate of 3 °C/min with an applied frequency of 1 Hz. Mechanical measurements were operated by DMA controlled-force test method.

Figure 3.13: TA Q800 Dynamic Mechanical Analyser

UV-Visible spectrophotometric analysis of P(BA-co-MMA)@PPy_1, P(BA-co-MMA)@PPy_2, P(BA-co-MMA)@PPy_3, P(BA-co-MMA)@PPy_4 nanofibers that were dissolved in DMF solvent, were carried out with UV-Visible Spectrophotometer (Perkin Elmer UV Visible Spectrophotometer, Figure 3.14).

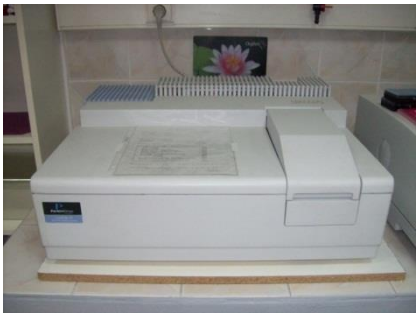

Figure 3.14: Perkin Elmer UV Visible Spectrophotometer.

Static contact angles of fiber surfaces under air were measured by using a KSV-CAM 200 contact angle meter with a PC controlled motorized syringe within ±1° precision (Figure 3.15).

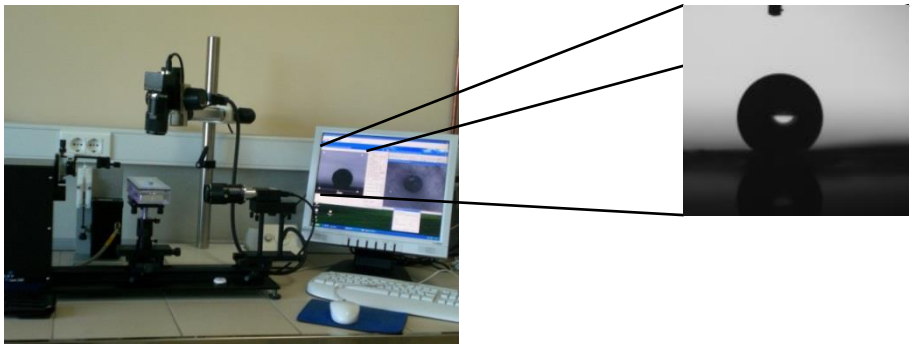

Figure 3.15: Contact Angle Meter, KSV CAM 200.

Real permittivity, imaginary permittivity and conductivity measurements of composite films were executed with Novocontrol broadband dielectric spectrometer (Alpha-A High Performance Frequency Analyzer, frequency domain 0.001 Hz to 3 GHz) at 25°C (Figure Samples were fixed between two copper electrodes with diameters of 20 mm (Figure 3.16).

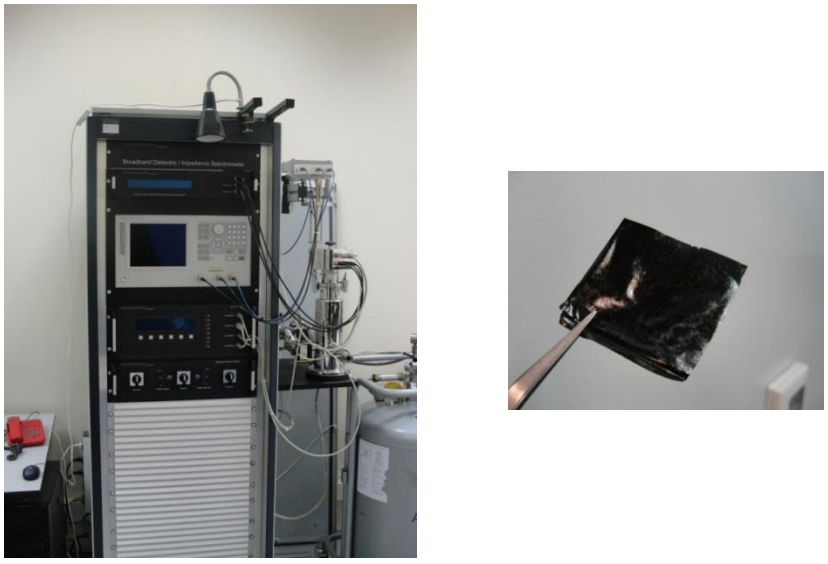

Figure 3.16: Novocontrol broadband dielectric spectrometer.

Resulting fibers were also characterized as morphologically by Scanning Electron Microscope (two diffrent SEM devices are used, firstly Philips XL30 and lastly, LEO SUPRA 35 VP) and the samples for the SEM measurements are prepared by coating of gold (Ion Sputter Metal Coating Device, MCM-100).

Number average (Mn) and weight average (Mw) molecular weights were determined in ultra pure THF solvent using Gel Permeation Chromatography (GPC) (Agilent 1200 series, BIC RID detector) equipment. The calibration was done by using the different molecular weight of PS standards (Mw=2000 to 800,000) and the passage time of the solvent was 0.3 mL/min.

4. RESULTS AND DISCUSSION

4.1 Copolymer and Composite Characterization

4.1.1 FTIR-ATR spectrophotometric analysis of P(BA-co-MMA)

The FTIR-ATR spectra P(BA-co-MMA) are shown in Figure 4.1 and it was recorded in the absorbance mode. Same figure shows the peaks at wave number of 2950 cm^{-1}, 1728 cm^{-1}, 1435 cm^{-1} and 1149 cm^{-1} which are assigned to CH stretching, C=O stretching, CH_3 stretching and O-CH_3 stretching vibrations, respectively. Polybutylacrylate (PBA) have similar molecular backbones, only slight differences can be found in their FTIR spectra. Absorption at 962 cm^{-1} was the characteristic peak of BA in P(BA-co-MMA) FTIR-ATR spectrophotometric results. These results are in agreement with literature [45].

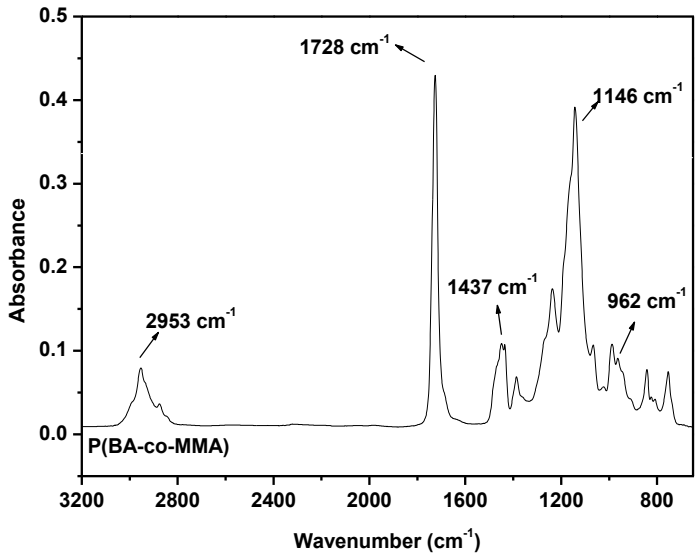

Figure 4.1: FTIR-ATR spectra of P(BA-co-MMA) fiber

Figure 4.1 shows the FTIR-ATR spectrums of prepared 5 wt % DMF solution for electrospinning solution, and obtained nanofibers from this solution.

Figure 4.2 shows the FTIR-ATR spectrums of prepared 5 wt % P(BA-co-MMA) in DMF solution which is used for electrospinning solution, and obtained nanofibers from this solution The peaks at 2855 cm^{-1}, 1728 cm^{-1}, 1437 cm^{-1}, 1146 cm^{-1} and 962 cm^{-1} are assigned to CH stretching, C=O stretching, CH_3 stretching, O-CH_3 stretching vibrations and the characteristic peak of BA, respectively in P(BA-co-MMA). However, new peaks are observed FTIR-ATR spectrum of 5 wt.% DMF solution at 1661 cm^{-1}, 1504 cm^{-1} and 657 cm^{-1} are belong to C=O stretching, C-N stretching and O=C-N stretching, respectively. These peaks are characteristic peaks for the pure DMF solvent.

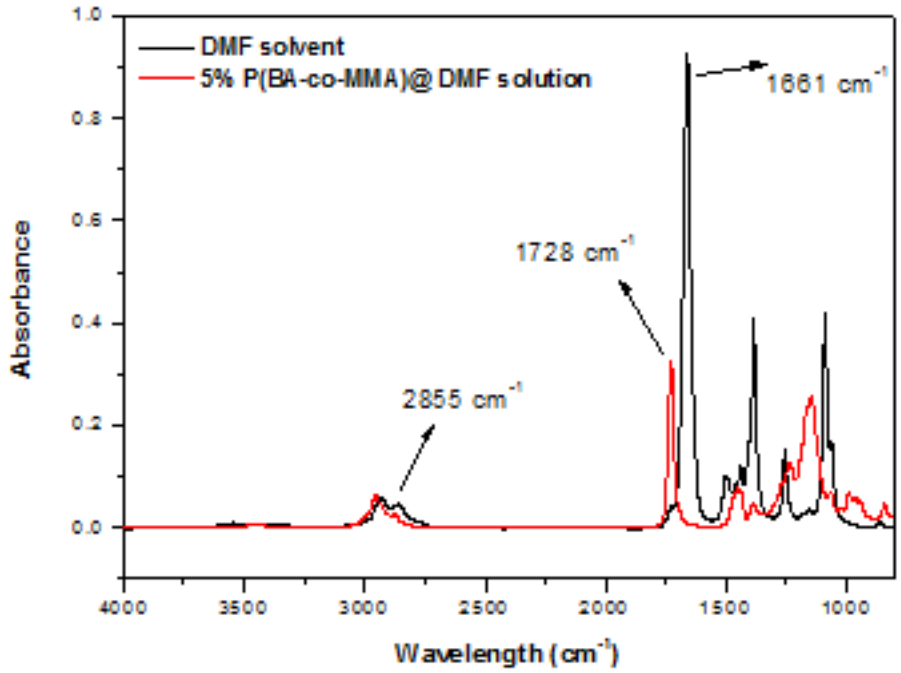

Figure 4.2: FTIR-ATR spectrums of prepared 5 wt. % DMF electrospinning solution, and DMF solvent.

5 wt.% of composites solved in DMF electrospinning solution. The CH_3 symmetric stretching mode can be observed at C-H stretching mode at 2855 cm^{-1}, C=O stretching mode at 1661 cm^{-1}, C-N stretching mode at 1504 cm^{-1}, O=C-N stretching mode at 657 cm^{-1} for peaks of DMF solvent [46].

The absorption bands appearing at 1661cm^{-1} was characteristic of C=O stretching of DMF. Also, C-H stretching of DMF at 2855 cm^{-1} can be seen as a strong peak. DMF characteristic peaks disappear after the electrospinning process due to the solvent evaporates during the electrospinning which was proved by FTIR spectra of obtained nanofibers from this solution. FTIR-ATR spectra of 5% wt. P(BA-co-

MMA) at DMF solution different from peak which at 1729 cm^{-1} is assigned to C=O stretching in P(BA-co-MMA). Increase in CN absorbance band at 1448 cm^{-1} corresponding to the increase in Py feed ratio was observed, and increase in C-H in plane vibration at 1140 cm^{-1}.

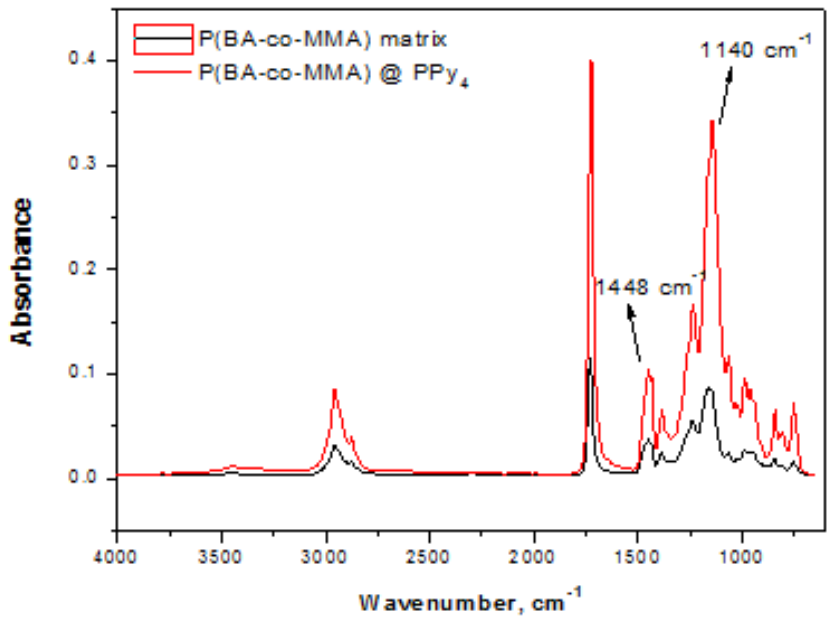

Figure 4.3: FTIR-ATR spectra of P(BA-co-MMA) fiber and P(BA-co-MMA)/PPy

PPy has interactions with carbonyl (C=O), and O-CH_3 groups of P(BA-co-MMA) as a result of chemical polymerization.

Approximately same stretching frequencies observed in the FTIR for P (BA-co-MMA) as well as for P(BA-co-MMA)/PPy composites. Due to the coinciding of peaks, FTIR might have not given different stretching frequencies in the composite. Therefore, as FTIR did not show much variation in their stretching frequencies for the P(BA-co-MMA) and P(BA-co-MMA)/PPy composite, it implies that weak interaction due to the low content of PPy and more ordered arrangement of the copolymer and the composite [47]. Thus, increase in CN absorbance band at 1448 cm^{-1} corresponding to the increase in Py feed ratio was observed. These results shown figure 4.4.

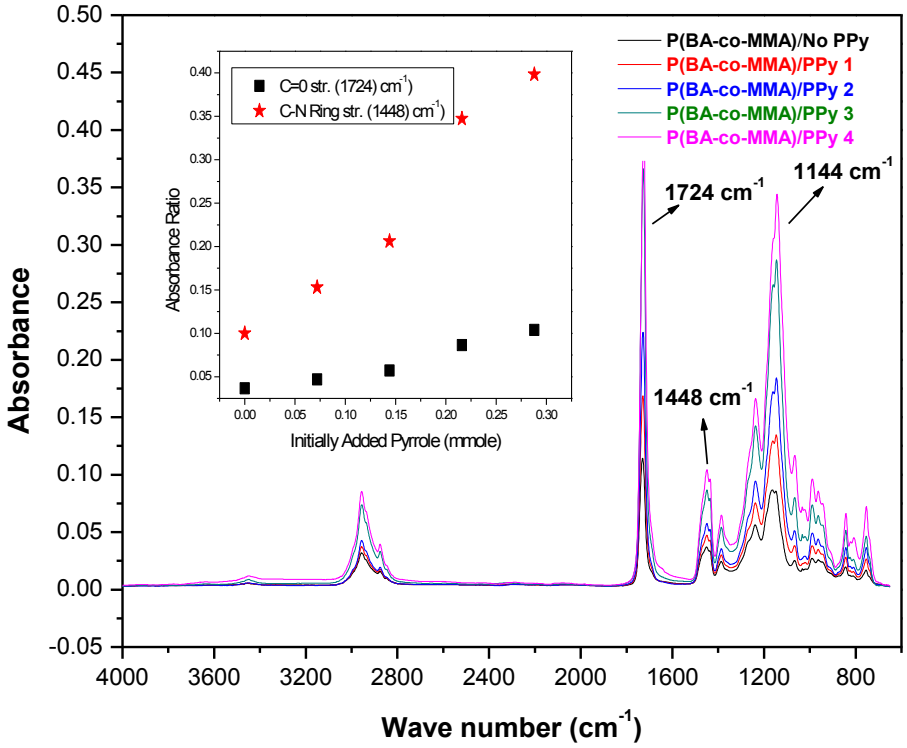

Figure 4.4 Effect of PPy content in P(BA-co-MMA) on FTIR -ATR absorbances

Effect of pyrrole content on composite films was investigated by FTIR spectroscopy and corresponding changes in absorbance values with pyrrole derivatives were evaluated. The characteristic bands of PPy ring vibration (C–C stretching) can be observed at 1382 cm^{-1}, C–H in plane vibration at 1021 and 1048–1235 cm^{-1},

C–N stretching vibration at 1448 cm^{-1}, C–H out of plane vibration at 840-846 cm^{-1} [47]. PPy has interactions with carbonyl (C=O) groups of P(BA-co-MMA) as a result of chemical polymerization. The carbonyl (C=O) groups play a significant role on the interactions between those segments (C=O and CN) and PPy cationic sites, 1729 cm^{-1} is assigned to C=O stretching in P(BA-co-MMA). Also, introduction of PPy into the P(BA-co-MMA) matrix, significant increase was observed in O-CH_3 vibrations at 1144 cm^{-1} (Figure 4.4).

4.2 UV- Visible Spectrophotometric Analyses

0.1 g dissolved nanofibers in 10 ml DMF (as shown in Figure 4.6) and then were analysed by UV-visible spectrophotometer (Figure 4.5). Nanofiber solution concentration was kept constant for every measurements of composites. UV-Vis spectroscopy of polypyrrole shows an absorbance maxima at about 480 nm in figure 4.5. This peak has been attributed to transitions of the valence to polaron and bipolaron/polaron states [48].

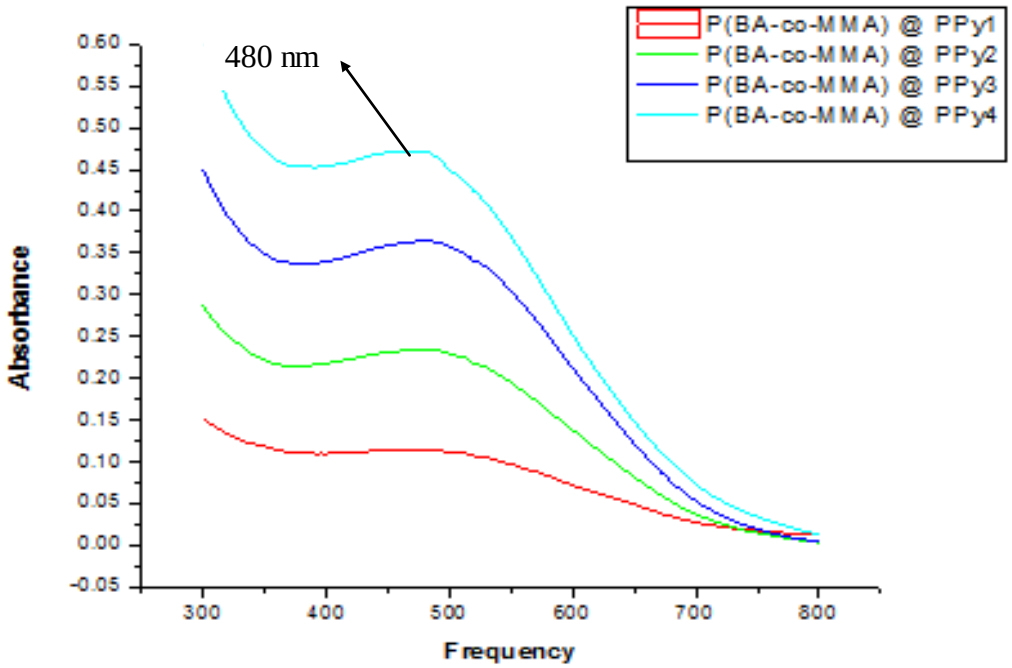

Figure 4.5: UV-Vis Spectrum of P(BA-co-MMA)@PPy_1, P(BA-co-MMA) @PPy_2, P(BA-co-MMA)@PPy_3, P(BA-co-MMA)@PPy_4 composite nanofibers dissolved in DMF

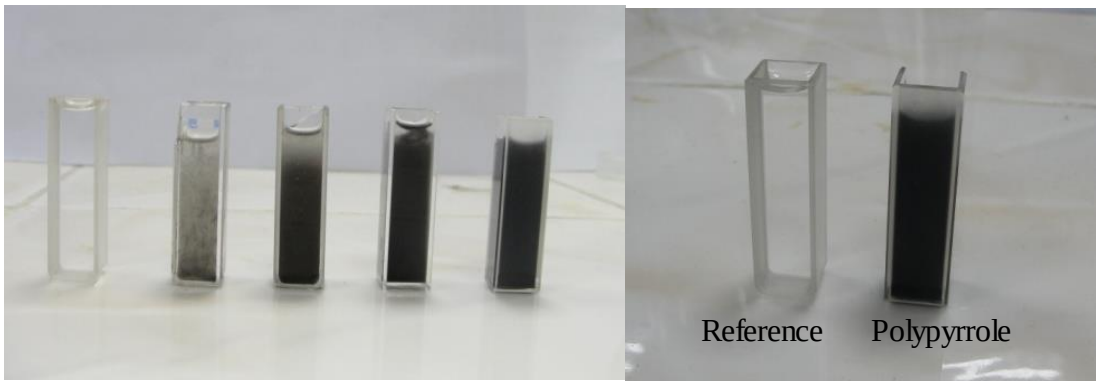

Figure 4.6: Dissolved nanofibers of P(BA-co-MMA)@PPy_1, P(BA-coMMA)@PPy_2 P(BA-co-MMA)@PPy_3, P(BA-co-MMA)@PPy_4

Relationship between, FTIR-ATR and UV-Vis results were shown in the figure 4.7. An increase in the FTIR absorbance values of PPy at 1448 cm^{-1} was observed corresponding to PPy wt% feed ratio and also same trend was occurred in the UV-Vis measurement due to incease in the maximum point of the peak at 480 nm related to Py characteristic peak at UV-Vis spectrum. Correlation of these results depicted in Figure 4.7.

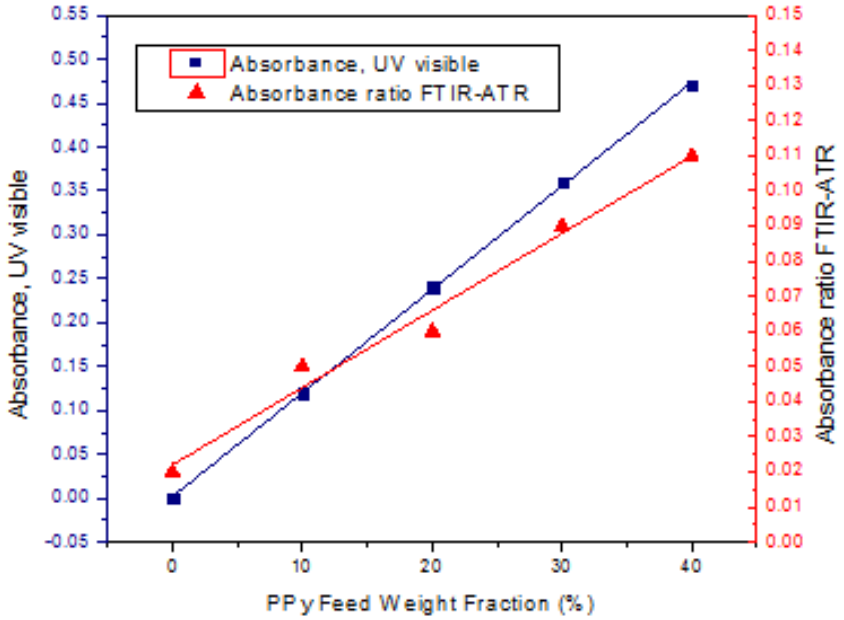

Figure 4.7: Correlation between FTIR-ATR absorbance ratio of CN str. ($1448cm^{-1}$) UV-Visible spectrophotometric absorbance values at 480 nm and Py feed weight fraction

4.3 Nuclear Magnetic Resonance (NMR) Spectroscopy of P(BA-co-MMA) Composites

Figure 4.8 shows the 1H-NMR spectra of copolymers recorded in deuterated $CDCl_3$ using TMS as the internal standard. The peak at δ=3.99 ppm is due to the $–OCH_2$ groups of BA and the peak at δ=3.64 ppm is due to $–OCH_3$ group of MMA. Observing other peaks δ=2.03 ppm due to α-CH, at δ=1.38 ppm $-2CH_2-$, at δ= 1.57 ppm $-3CH_2-$ and δ=0.91 ppm due to the $-4CH_3-$ of n-butyl acrylate and δ=1.08 ppm and δ=1.22 ppm to $α-CH_3$ of methyl methacrylate, respectively and δ=7.24 ppm is due to $CDCl_3$. Moreover, a peak is observed at δ=3.46 is due to ethanol in remaining copolymer structure.

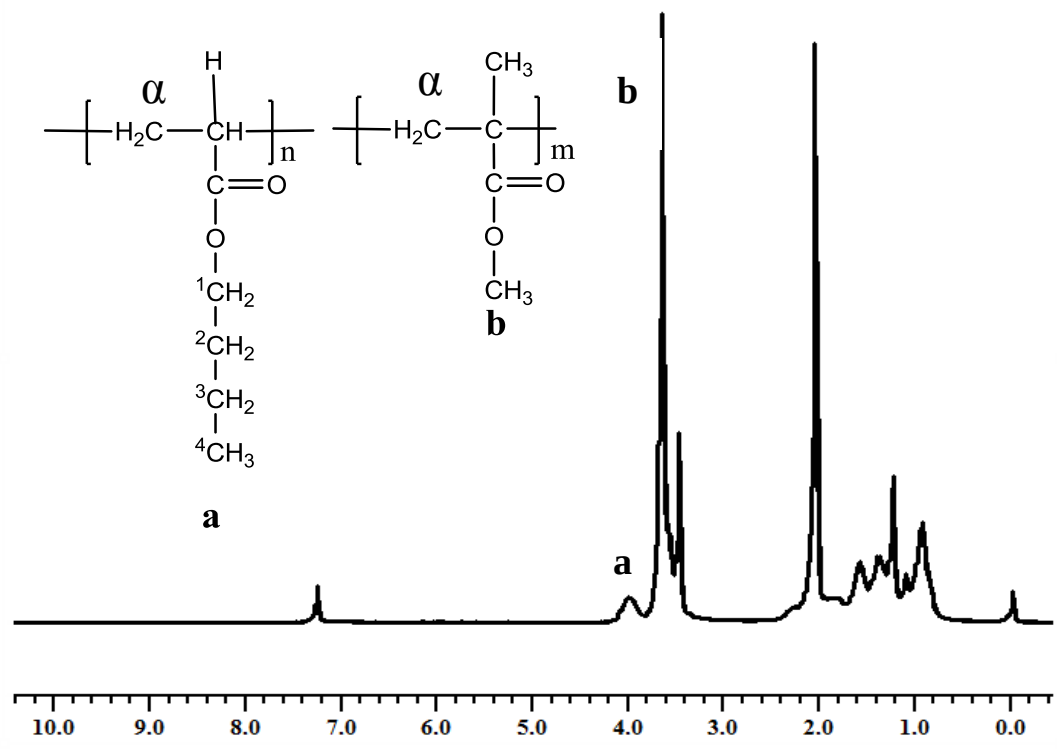

Figure 4.8: 1H-NMR spectra of copolymers recorded in $CDCl_3$

The quantatity of MMA and BA in the copolymers was calculated from the integral ratio of methyl protons (-$COOCH_3$) and methylene protons (-$COOCH_2$) originated from MMA and BA respectively and these peak domains included methyl and methylene protons obtained from 1H-NMR spectrum in agreement with the literature [49]. The mole fraction of MMA in the copolymer (FMMA) can be determined using the following relationship

$$F_{MMA} = \frac{2A(-OCH_3)}{2A(-CH_3)+3A(-OCH_2)} \quad \textbf{(4.1)}$$

Where A(-OCH_3) and A(-OCH_2) stand for the total peak areas of -OCH_3 and -OCH_2, respectively. A(-OCH_3) was shown in Figure 4.9 and FMMA calculated as 0.821; A(-OCH_2) was shown in Figure and FBA calculated as 0.178 [45] .

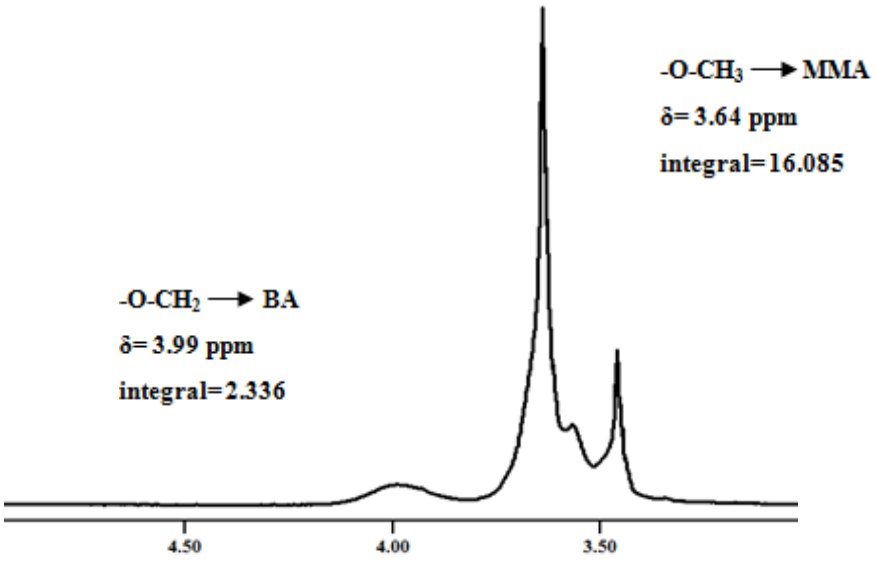

Figure 4.9: NMR Spectrum of P(BA-co-MMA) (0.0-5 ppm)

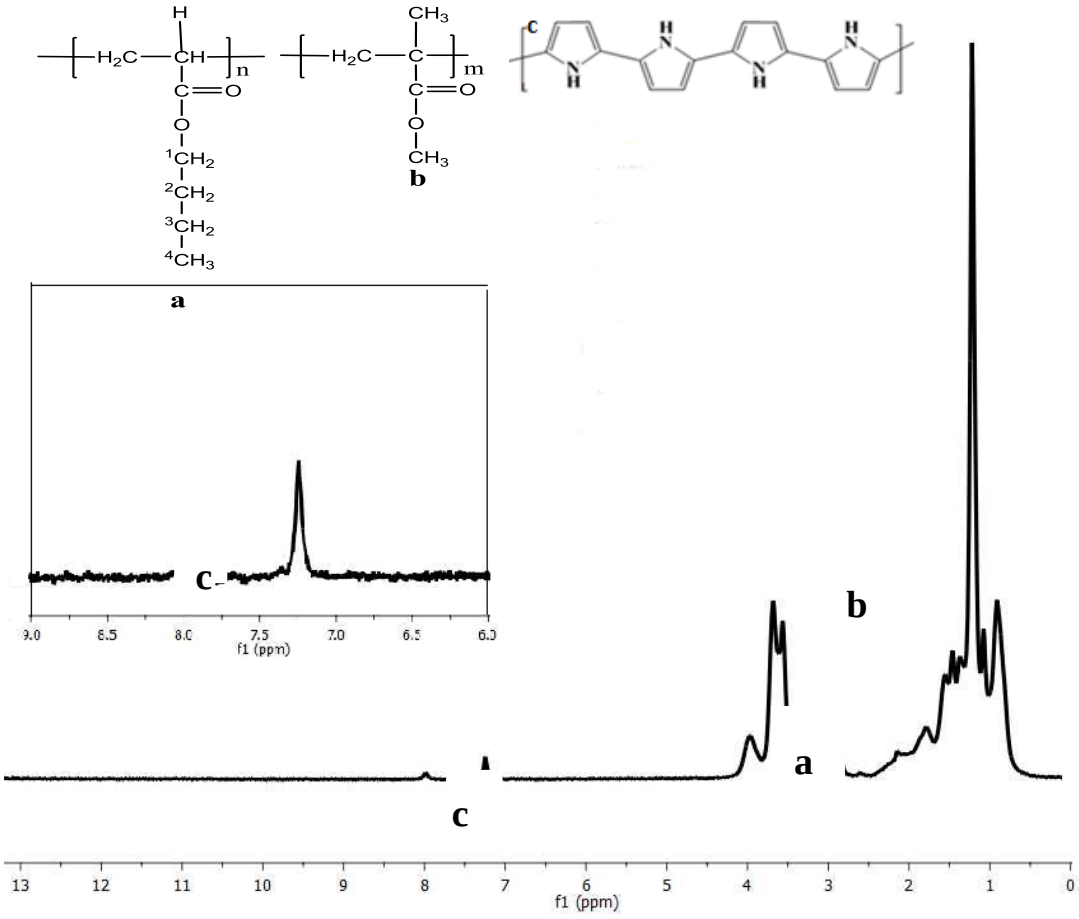

Figure 4.10: NMR Spectrum of P(BA-co-MMA)@PPy$_4$

Polypyrrole is insoluble in DMSO, while P(BA-co-MMA)/PPy polymer can be dissolved in several organic solvents such as DMF and DMSO. P(BA-co-MMA)/PPy solution in $CDCl_3$ is giving $CDCl_3$ peak at 7.24 ppm PPy displays a new peaks at 8.0–8.1 ppm which is assigned to hydrogens in PPy rings [50]

4.4 Contact Angle Measurement P(BA-co-MMA) and P(BA-co-MMA)/PPy Copolymer Composites

Increasing the pyrrole content of composite should have an effect on the contact angle due to the pyrrole content on nanofiber surface. The expectation is, higher the pyrrole content, higher the contact angle (Table 4.1) number of nanofibers and micro beads appear on the pyrrole 4 structure and such a micro-nano hierarchical structure (Figure 4.11) leads to a high hydrophobicity with a contact angle of 152°.

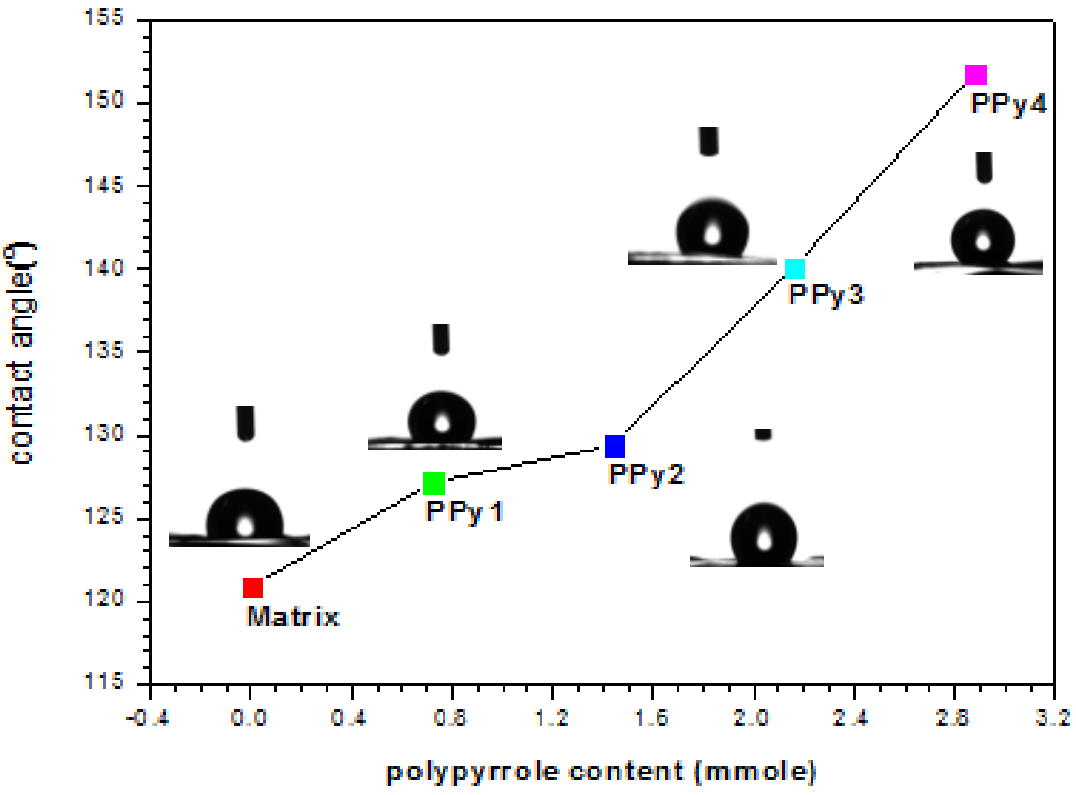

Figure 4.11: The relationship between contact angle and diameter of nanofibers for P(BA-co-MMA) and different moles of pyrrole(feed)

Table 4.1: Results of contact angle for nanofibers

Component	**Contact angle (°)**	**Diameter** (nm)
P(BA-co-MMA)	122	600
P(BA-co-MMA)@PPy$_1$	127	463
P(BA-co-MMA)@PPy$_2$	129	379
P(BA-co-MMA)@PPy$_3$	140	342
P(BA-co-MMA)@PPy$_4$	152	263

4.5 Effect of Different Feed Concentration of Pyrroles on Nanofibers

P(BA-co-MMA) matrix and composite samples have been prepared, changing the concentration of addition pyrrole at P(BA-co-MMA) in DMF. In this section, concentration effects on the diameters of nanofibers were examined. Therefore electrospinning parameters have been hold same for all solution. Morphologic properties of these polymers were shown in SEM and images in figure 4.12

Table 4.2: Standart deviation values and average nanofiber diameters

Component	**Diameter** (nm)
P(BA-co-MMA)	600± 93
P(BA-co-MMA)@PPy$_1$	463± 51
P(BA-co-MMA)@PPy$_2$	379± 42
P(BA-co-MMA)@PPy$_3$	342± 35
P(BA-co-MMA)@PPy$_4$	263± 50

Mole percent of the initially added Py concentration varies from 0.072 to 0.144 the corresponding average diameters of the nanofibers are reduced from 463 to 263 nm (Table 4.2). With the increase of the initially added Py concentrations, some beads begin to appear. This may be a result of the increased PPy content in the electrospinning solutions.

Morphological analysis of nanofibers without pyrrole and pyrroles are presented in figure 4.13 . The average diameter of electrospun fibers of different concentrations is determined by using Image J program to randomly measure the diameters of 85 individual fibers shown in SEM images with x3000 magnitude. As pyrrole content in electrospun nanofibers increased it was found that the average diameter was decreased as shown in figure. The decrease in average diameter with the increase amount of pyrrole can explained by the conductivity nature of PPy.

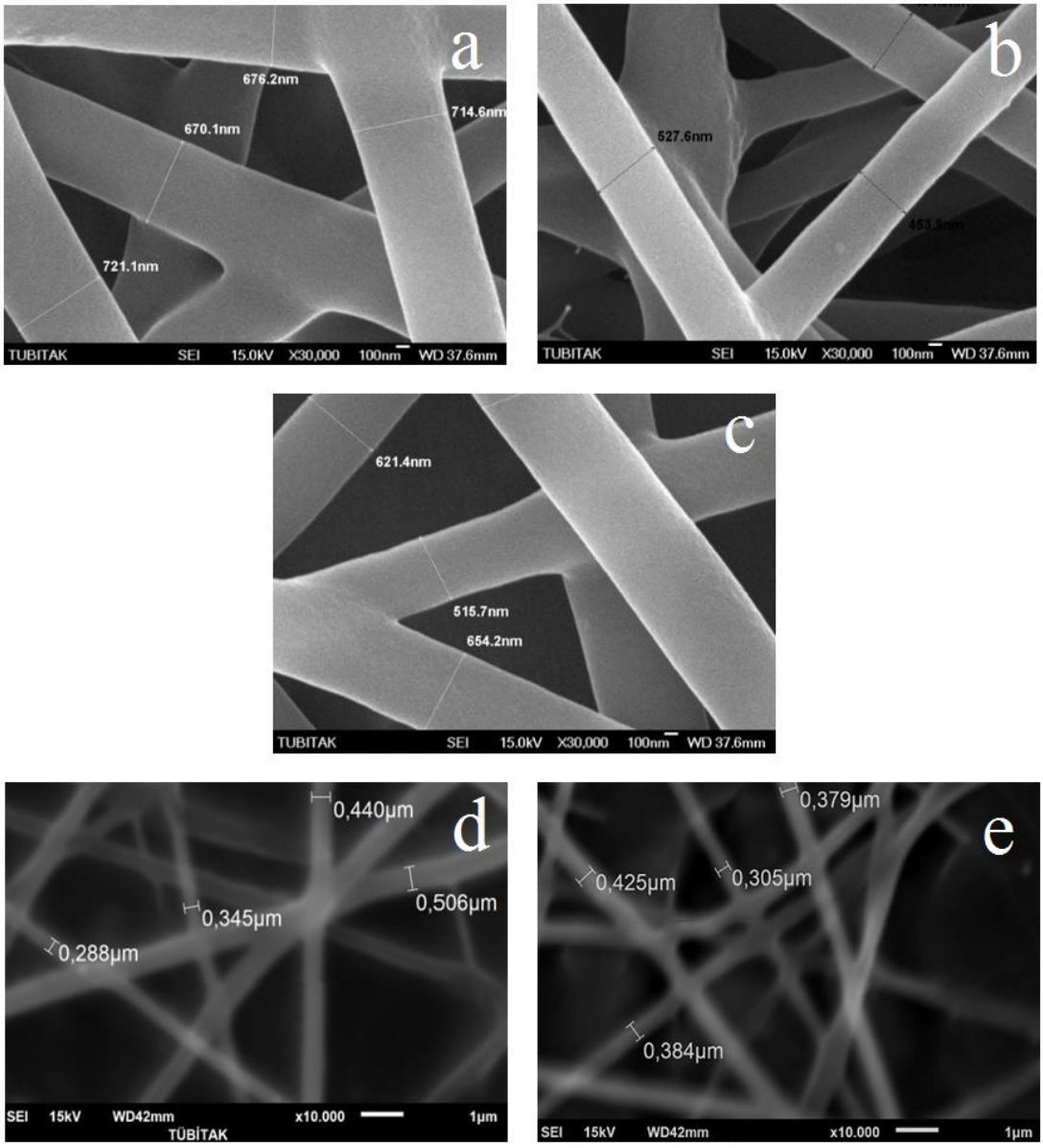

Figure 4.12: SEM images of the samples at different P(BA-co-MMA)/PPy (wt) concentrations a) 0% , b) 10%, c) 20%, d) 30%, e) 40%

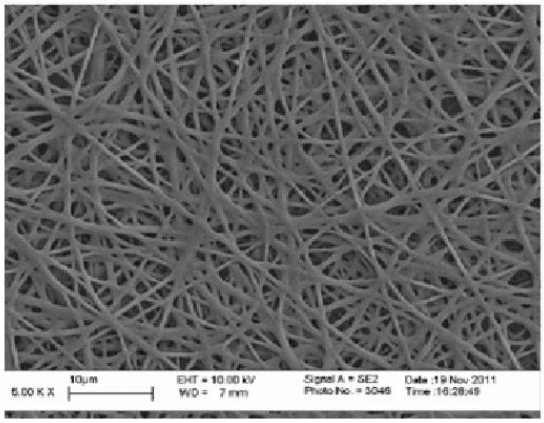
10µm
5.00 K X
EHT = 10.00 kV
WD = 7 mm
Signal A = SE2
Photo No. = 3046
Date :19 Nov 2011
Time :16:28:49

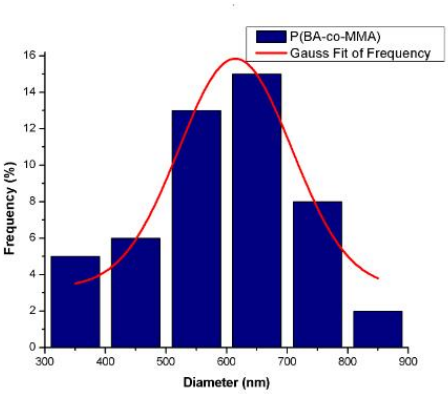
P(BA-co-MMA)
Gauss Fit of Frequency
Frequency (%)
Diameter (nm)

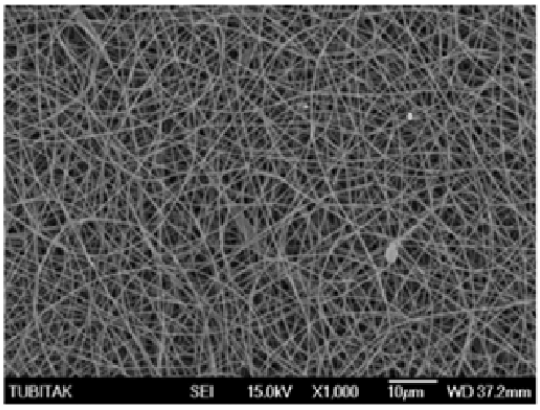
TUBITAK
SEI
15.0kV
X1,000
10µm
WD 37.2mm

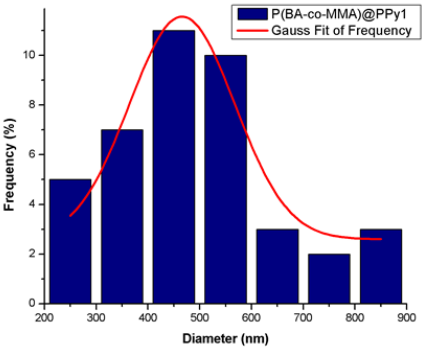
P(BA-co-MMA)@PPy1
Gauss Fit of Frequency
Frequency (%)
Diameter (nm)

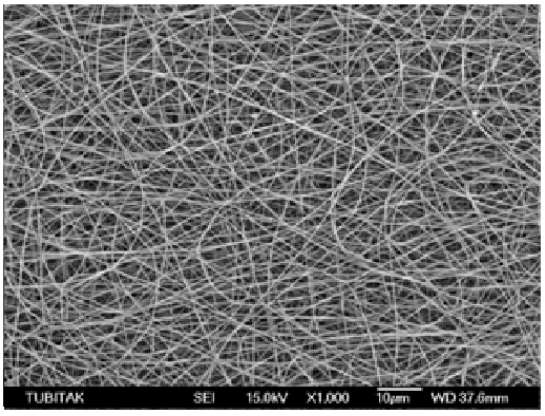
TUBITAK
SEI
15.0kV
X1,000
10µm
WD 37.6mm

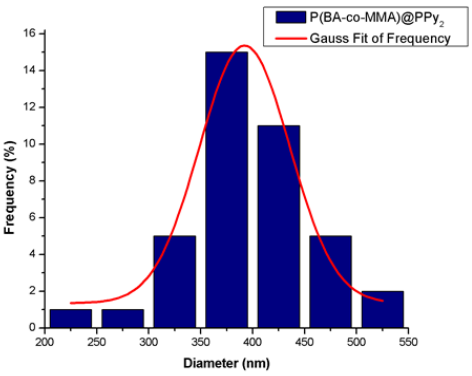
P(BA-co-MMA)@PPy2
Gauss Fit of Frequency
Frequency (%)
Diameter (nm)

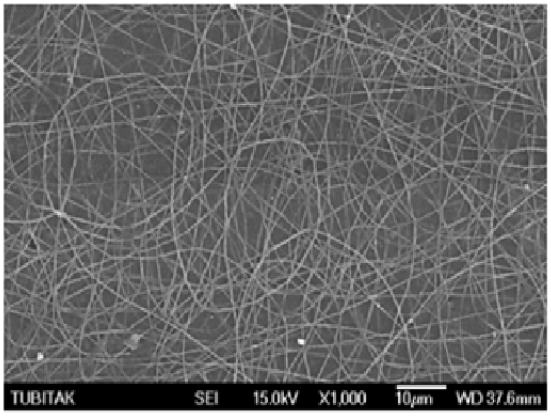
TUBITAK
SEI
15.0kV
X1,000
10µm
WD 37.6mm

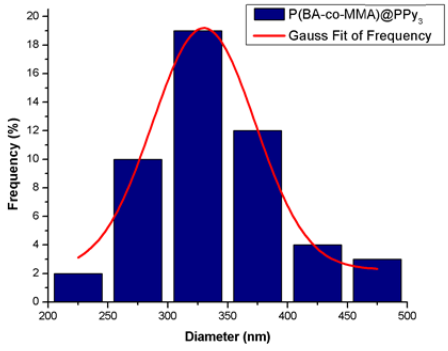
P(BA-co-MMA)@PPy3
Gauss Fit of Frequency
Frequency (%)
Diameter (nm)

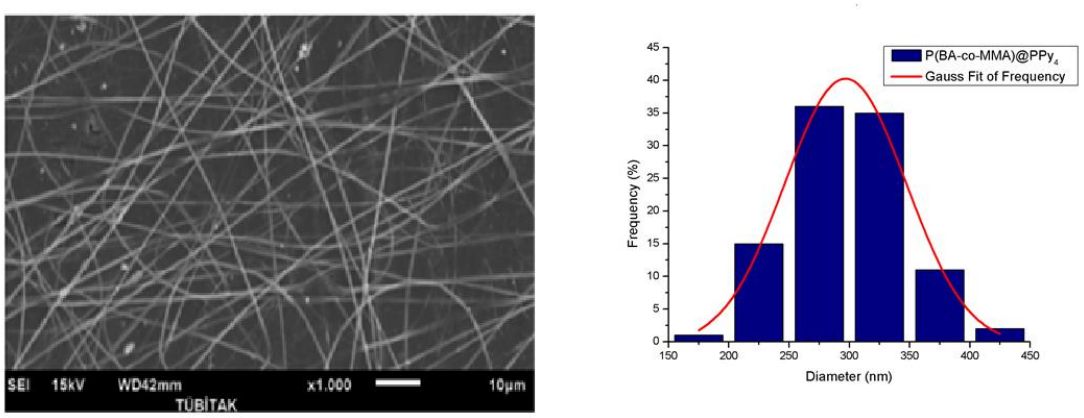

Figure 4.13: SEM images of P(BA-co-MMA) nanofibers and P(BA-co-MMA) nanofibers with 10wt%, 20 wt%, 30 wt%, 40 wt% PPy, and distribution of the diameters of nanofibers

4.6 Effect of Flow Rate on Nanofiber

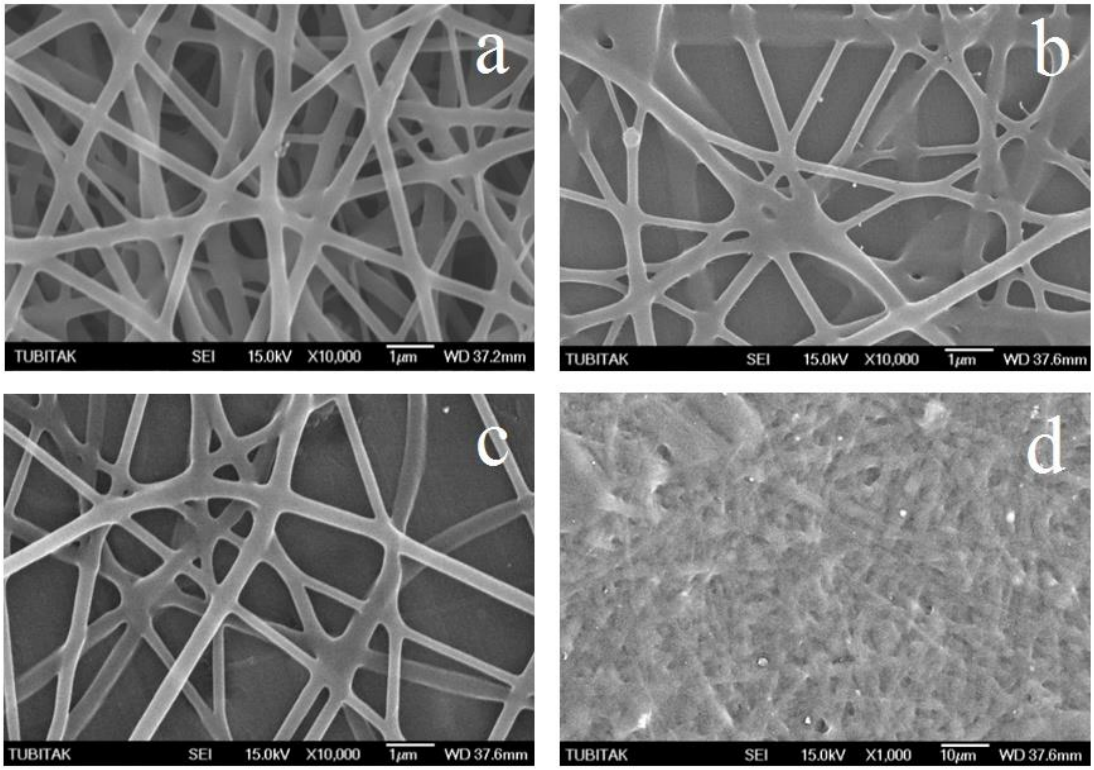

Figure 4.14: SEM images different flow rates P(BA-co-MMA)/PPy fibers a)1ml/h, b) 3ml/h c) 5ml/h d) 7ml/h

The feedrate will determine the amount of solution available for electrospinning. When the feedrate is increased, there is a corresponding increase in the fiber diameter or beads size. As figure 4.14 shows that higher flow rates prevent the

fibers. Reversely figure a and b show that more lower flow rates easily formation of fibers. Figure also shows that the morphology of the electrospun P(BA-co-MMA).

4.7 Effects of Dielectric Constant of Solvent Mixture on Nanofiber

In order to determine an optimum solvent system for electrospinning P(BA-co-MMA), different single and solvent mixture systems were studied. Three solvents with different electrical conductivities were used to prepare P(BA-co-MMA) solution at a fixed polymer concentration of 5 wt %. Dielectric constant values of Solvent mixture were calculated by the following equation;

$$\varepsilon_m = \varepsilon_1 x_1 + \varepsilon_2 x_2 \qquad \textbf{(4.2)}$$

where ε_1 is the dielectric constant of the solvent and x_1 is the corresponding volume fraction.

Table 4.3: The dielectic effect of further solvent mixtures on fiber formation solution mixtures consisting of DMF and THF

Component(5% (w/v))	**Solvents (%)**	**Dielectric Constant**	**Diameter (nm)**
P(BA-co-MMA)/PPy	DMF	36.71	370± 93
P(BA-co-MMA)/PPy	THF	7.47	670± 51
P(BA-co-MMA)/PPy	DMF/THF (20/80)	13.32	490± 42
P(BA-co-MMA)/PPy	DMF/THF (80/20)	30.86	380± 35

Dielectric constants of different solvents and diameter of resulting nanofibers prepared in these solvents shown in Table 4.3 and also shows the nanofiber diameters obtained from scanning electron microscopy (SEM) images of P (BA-co-MMA) nanofibers electrospun from 5% (w/v) P(BA-co-MMA) solution in different solvents (DMF, THF). Bead-free nanofibers can be obtained for the polymer solutions having high dielectric constant. Table 4.3 shows the nanofibers of 5% DMF solution. It has the lowest diameters of nanofibers among the others due to its

highest dielectric constant. Figure 4.15 shows the beaded nanofibers of THF solution which has the highest diameters of nanofibers due to its lowest dielectric constant. THF/DMF % (80/20) mixture has the low dielectric constant compared to others except THF, so it exhibited the higher fiber diameters.

Increase in the DMF content causes an increase in dielectric constant which results a decrease in the fiber diameter and improve the fiber morphology. These results are in agreement with in literature .

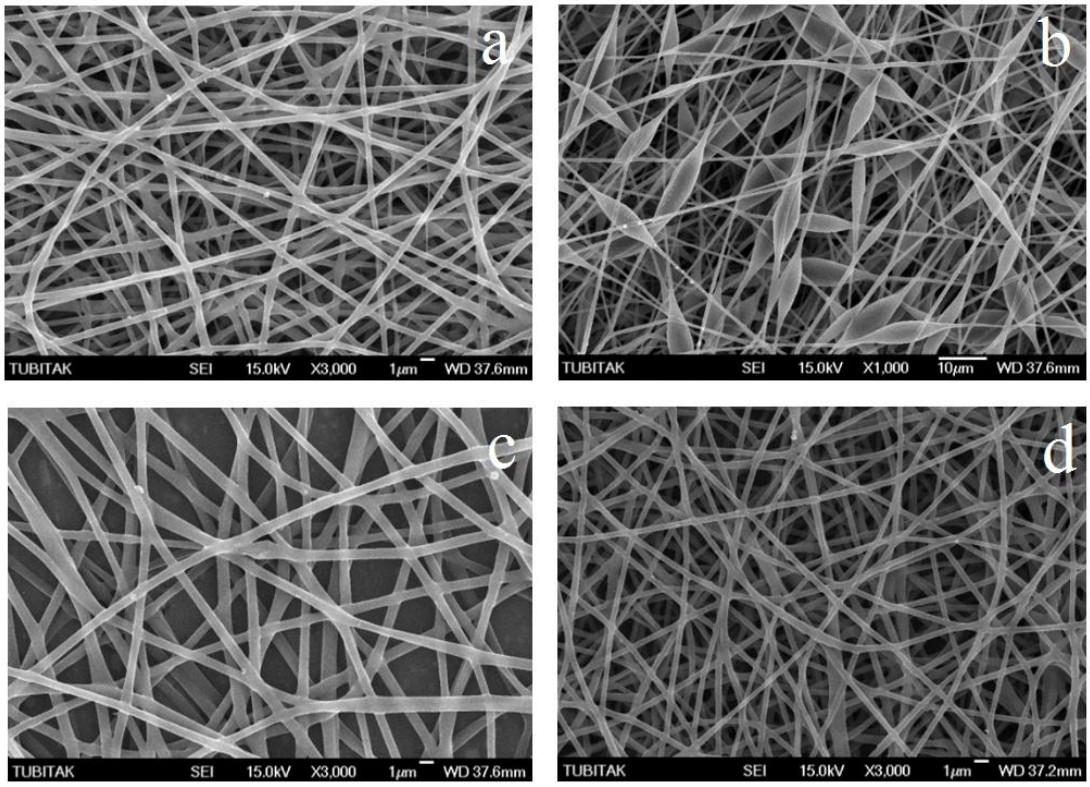

Figure 4.15: SEM images of- nanofibers from (a) 100% DMF solution (b) 100% THF solution (c) THF/ DMF (20/80%v) solution (d) THF/DMF (80/20%v) solution mixtures.

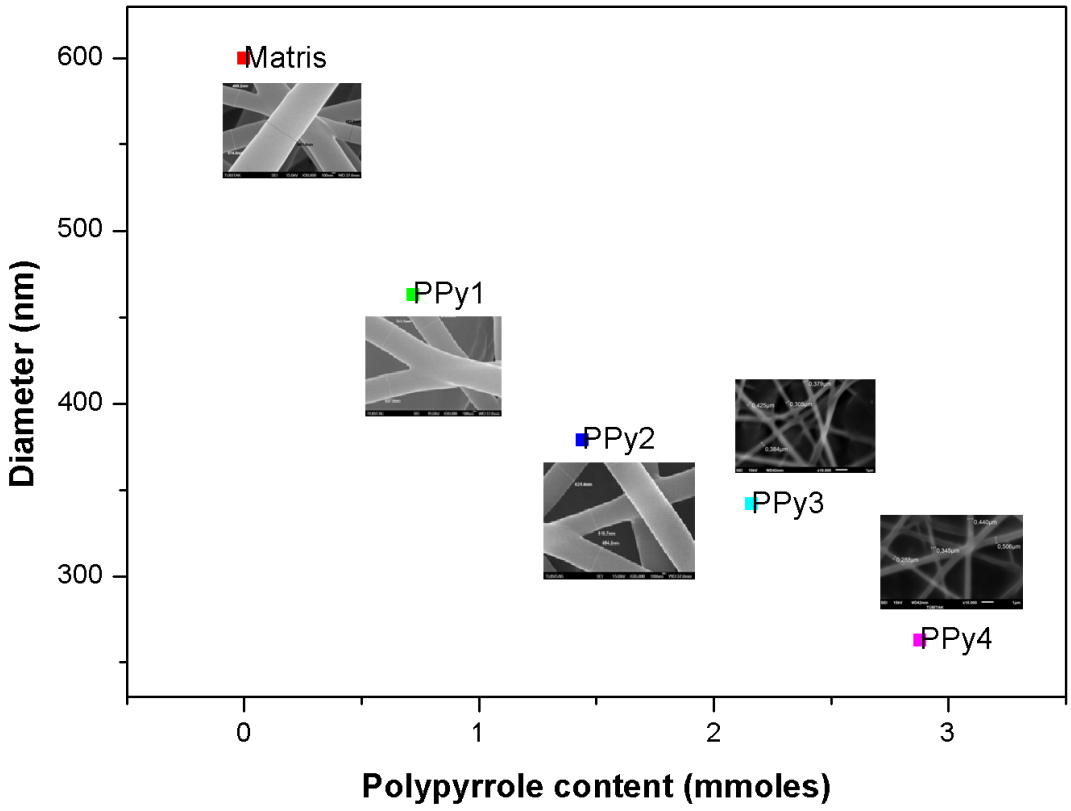

Figure 4.16: Relationship between diameter of nanofiber coatings and content amount of polypyrroles.

In addition to these measurements, the particle size of polypyrrole/ n-butyl acrylate-co-methyl methacrylate composite was investigated. Unfortunately particle size measurement could not be done because polypyrrole/ n-butyl acrylate-co-methyl methacrylate composite can not dissolved in instrument'ssolvent and the particle size measurement instrument can not detect un-solved composites. The composites should be able to dispersed with instrument's solvent in order to measure the particle size**.**

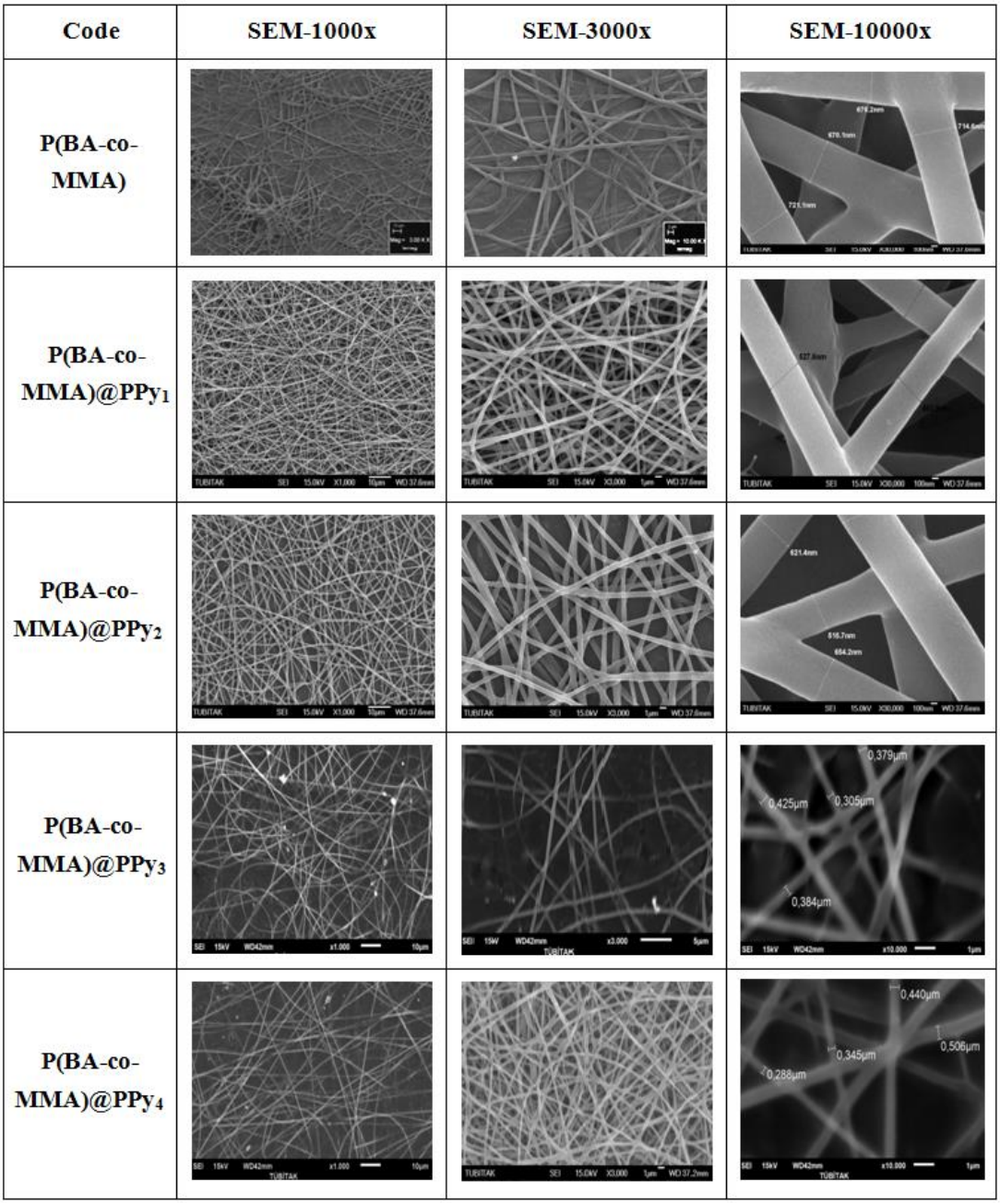

Figure 4.17: SEM images of Poly(BA-co-MMA) composites

4.8 Molecular weight determination

Mn and Mw results obtained from GPC are given in Table 4.4. Polydispersity index (PDI) of copolymers which were calculated from (Mw/Mn).

Table 4.4: Mn, and Mw values of the copolymers from GPC

Copolymer	M_w **(g/mol)**	M_n **(g/mol)**	**PDI**
P(BA-co-MMA)	663000	518000	1.29

Table 4.5: Intrinsic viscometric measurement

Component	η^a **(dL/g)**
P(BA-co-MMA)	2.94
P(BA-co-MMA)@PPy_1	2.91
P(BA-co-MMA)@PPy_2	2.69
P(BA-co-MMA)@PPy_3	1.70
P(BA-co-MMA)@PPy_4	1.07

η^a Determined from Ubbelohde-type viscometer

The correlation between nanofiber diameters, viscosity and PPy feed ratio was examined. With the decrease of intrinsic viscosity of polymers, low average nanofiber diameters were obtained. The low average nanofiber diameters probably result from the relatively low molecular weight of conductive polymers **]. Therfore, PPy creates decrease in viscosity and that causes the smaller diameter of nanofibers. Moreover, Nanofibers have small average diameters related to the electropinning solutions that have higher conductivity as sown in figure 4.18.

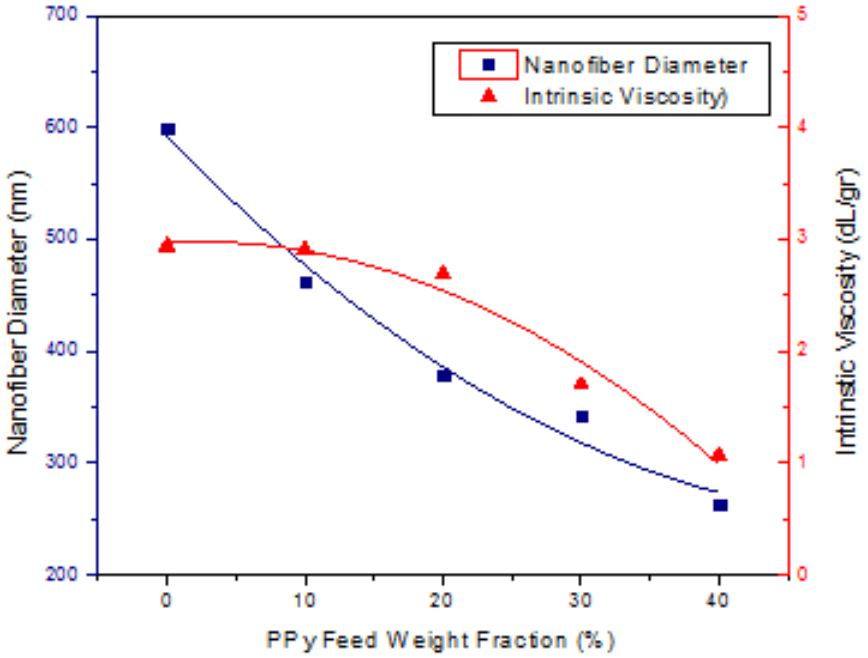

Figure 4.18: Relationship between nanofiber diameter, intrinsic viscosity and PPy feed weight fraction of composites

4.9 Dynamic Mechanical Analysis of Composites

Figure 4.19 shows the stress-strain curve of polymers that were obtained by DMA. The area under the stress-strain curve is known as toughness, which represents the total strain energy per unit volume in the material induced by the applied stress

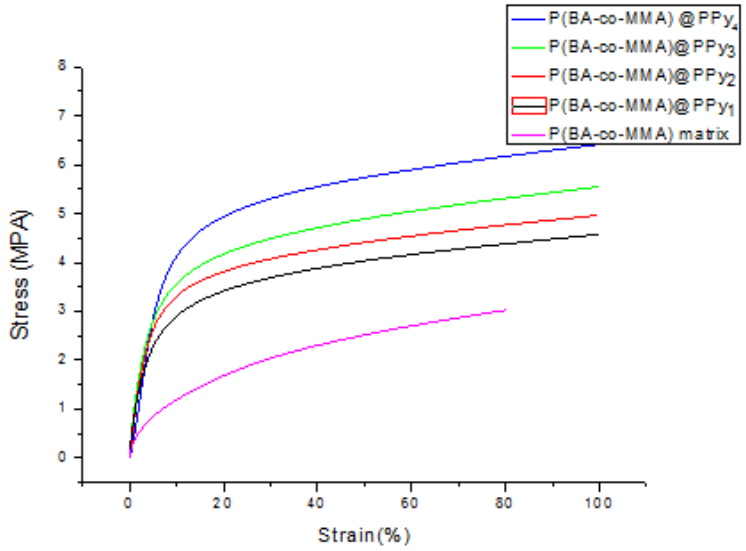

Figure 4.19: Stress-strain curve of polymers that were obtained by DMA

It was seen that the toughness increases with increasing content of polypyrroles in the composites. Increase in toughness was indicated in Table 4.6.

Table 4.6: Toughness of polymers that were obtained by DMA.

Sample	**Toughness (N/mm2)**
P(BA-co-MMA)	3.80
P(BA-co-MMA) @PPy1	4.17
P(BA-co-MMA) @PPy2	4.63
P(BA-co-MMA) @PPy3	5.37
P(BA-co-MMA) @PPy4	7.29

4.10 Tg Determination by Dynamic Mechanical Analyser, DMA

The DMA gives information about glass transition (Tg) and viscoelastic properties of polymeric amorphous materials. Under tension/compression deformations the measured viscous component is referred to as the loss modulus (E"), while the measured elastic component is referred to as the storage modulus (E').

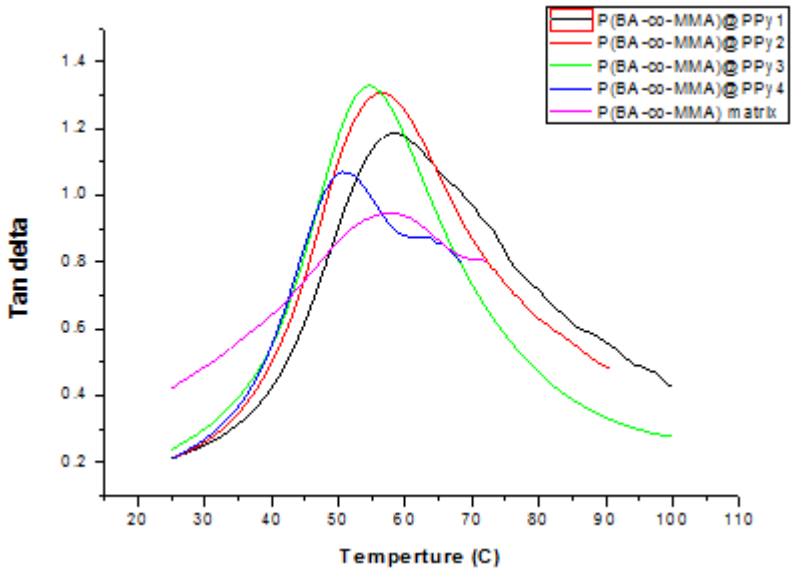

Figure 4.20: Tg values of composites obtained by DMA.

The ratio of the loss modulus to the storage modulus is referred to as the loss tangent (E"/E'), or tan delta. Tg of the composites is located as the temperature where tan delta is maximum. Figure 4.20 shows tan delta change vs. temperature where figure 4.21 shows tan delta peak change vs. pyrrole content. Table 4.7 shows the peak Tg values explicitly.

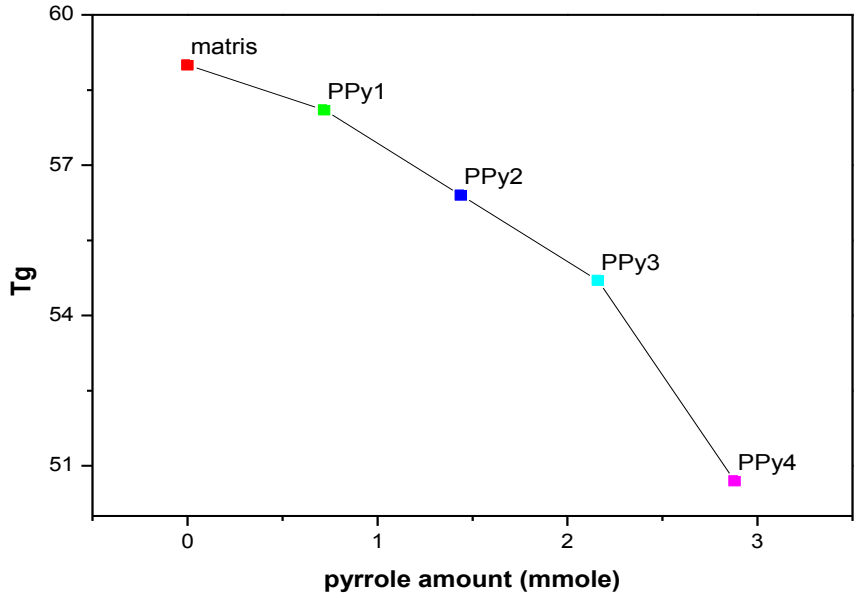

Figure 4.21: Correlation between Tg values and Pyrrole amount.

Table 4.7: Tg valuesof composites with different pyrrole amounts.

Sample	**Tg values (C)**
P(BA-co-MMA) matrix	58.1
P(BA-co-MMA) @PPy$_1$	57.3
P(BA-co-MMA) @PPy$_2$	56.4
P(BA-co-MMA) @PPy$_3$	54.7
P(BA-co-MMA) @PPy$_4$	50.7

4.11 Electrical Conductivity and Dielectric Behaviour

Electrical conductivity measurements were carried out at room temperature. The frequency dependent electrical conductivities (AC conductivity) of composite thin films were represented in Figure 4.22 . Linear correlation was observed between the absorbance values of CH in plane vibration peaks attained from FTIR-ATR and

conductivities from dielectric spectrometer. In order to show correlation, absorbance and conductivity values of composite thin films are plotted as a function of the initially added pyrrole derivative concentrations as an inset images. The amount of the conjugated polymer governs the ability of conductive network formation which is indicated by increase in conductivity of the composite. Also, conjugated polymer/pyrrole/matrix interactions (and partly DMF) and physical properties of the matrix influence. The homogenity of the dispersant phase which, in turn, affects the dielectric and conductivity properties of the composites. Well dispersion of reduced Cerium(IV) and PPy obtained by having conductive films were able to form a conducting network.

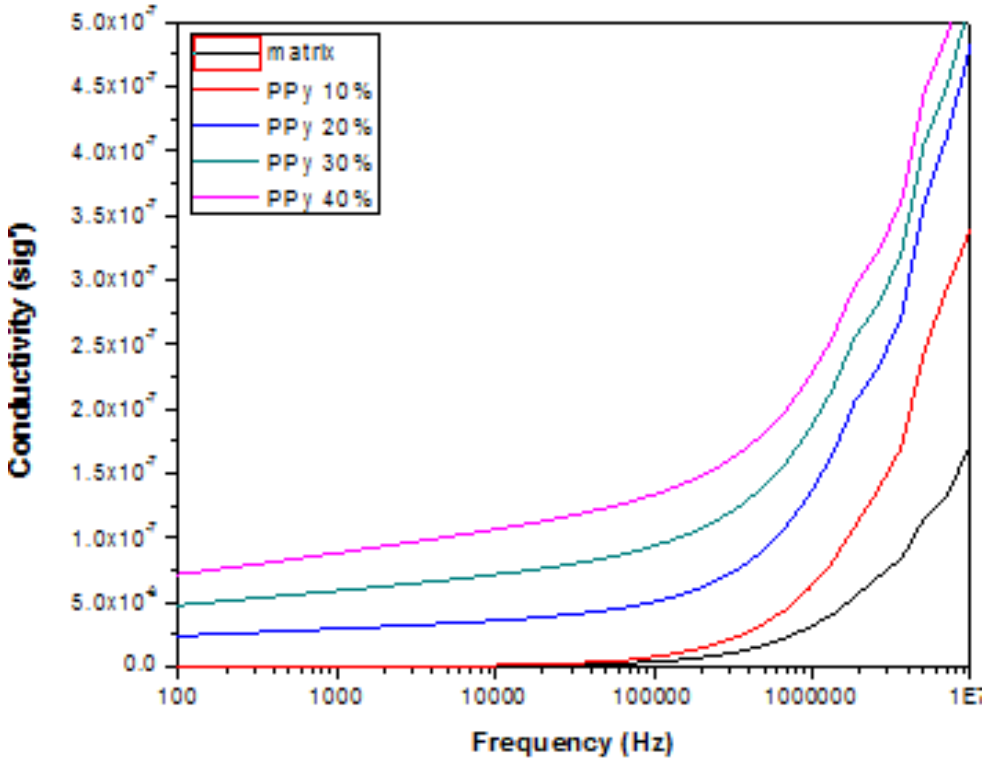

Figure 4.22: AC conductivity of composite films

It was also found that conductivity becomes larger by the increase of initially added Py. In addition, there were not much variation in the conductivity with frequency from 10^2 to 10^5 Hz and then at frequency range of 10^5-10^7 Hz, an obvious increase in the composite thin films conductivity with frequency was observed ,which is a common behavior for polymeric and semiconductor samples [48]. The first trend depends on available free charges in the composite films, where as for the second region which is frequency dependent conductivity is due to trapped charges

(formation of excess polaron and bipolaron- only active at higher frequency region) [51]. The dielectric behaviour of polypyrrole composite films was studied between 10^{-2}-10^{7} Hz as well.

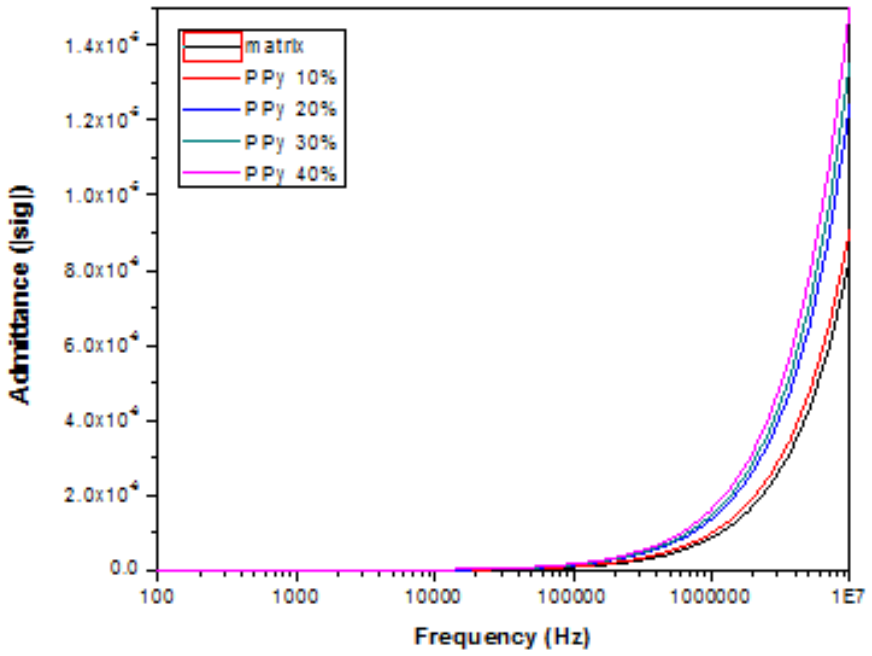

Figure 4.23: AC admittances of composite films.

Dielectric constant is reduced with increasing frequency for all composites, because interfacial electric dipoles cannot align themselves to the fast changing electric field direction. Kunanuruksapong and Sirivat, and Putson et al. reported that the dielectric constant decrease with increasing frequency due to decreasing interfacial polarization. Since PPy has high dielectric molecules [52] the dielectric constants of the polymers are increased with increasing PPy content.

All composites show approximately frequency independent conductivity up to 105 Hz. This can be caused by random diffusion of the charge carriers, via activated dopping [58]. After 10^{5} Hz, conductivity increases with increasing frequency. This cause of such phenomenon is explained by the formation of excess charge carriers (polaron and bipolaron) at frequencies $>10^{5}$ Hz [52].

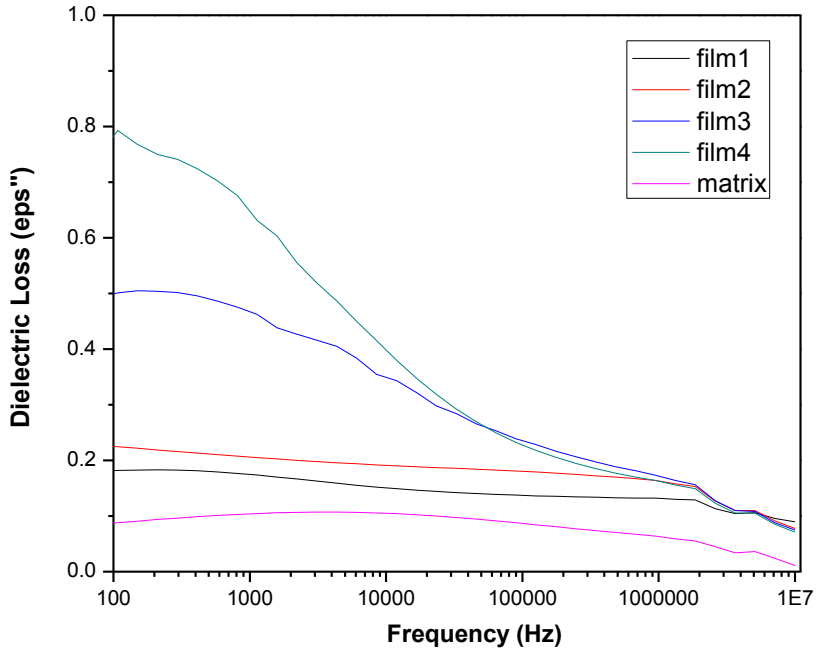

Figure 4.24: Frequency dependence dielectric loss of composite films.

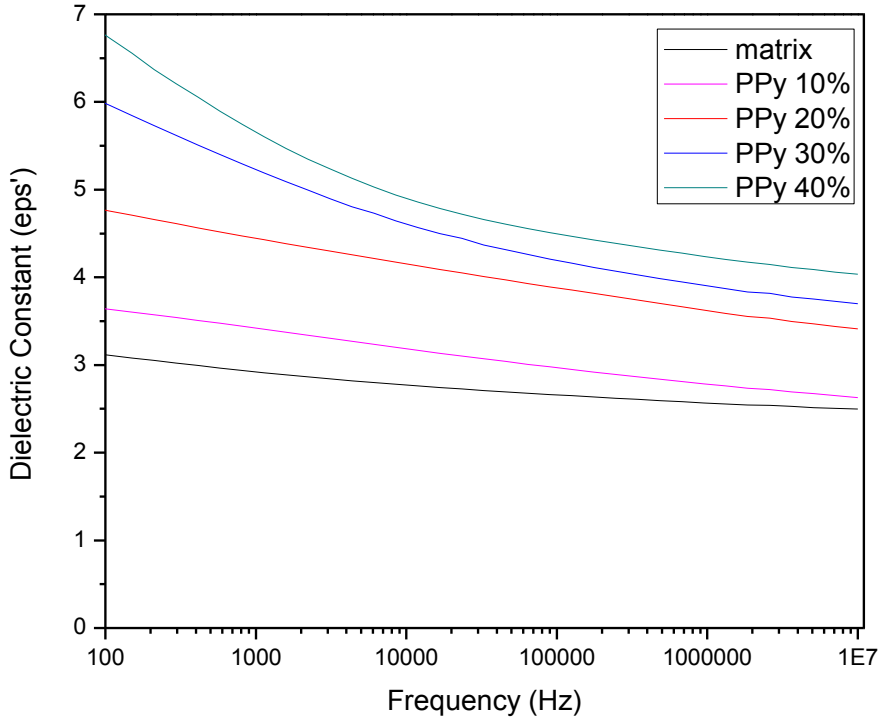

Figure 4.25: Frequency dependence dielectric constant of composite films.

Figure 4.24 and figure 4.25 show the dielectric constant (ε') and dielectric loss (ε'') graph different pyrrole composite films respectively. The dielectric constant and dielectric loss decreases with the increasing of frequency for all samples and also observed that, dielectric constant as well as dielectric loss values are higher for

higher PPy content in the composite films. When the dielectric values is compared with conductivity values it can be seen that the behaviour is opposite.

5. CONCLUSION

The objective of this thesis was to obtain nanofibers of n-Butyl Acrylate/Methyl Methacrylate copolymer by electrospinning method. Thus, first n-Butyl Acrylate/Methyl Methacrylate copolymer was synthesized by emulsion polymerization in aqeuos medium. Lately, pyrrole was added to matrix to achieve conductive composites. Nanofiber was evelauated by FTIR-ATR, UV-Vis spectra and especially NMR spectrum of P(AN-co-VAc)/PPy composites showed that Py had participated in polymerization

SEM images indicate that the diameters of P(BA-co-MMA) composites in different solutions. Dielectric constants of different solvents and diameter of resulting nanofibers was compared. High dielectric solvents such as DMF, lowest diameters of nanofibers among the others due to its highest dielectric constant. As opposite beaded nanofibers of THF solution which has the highest diameters of nanofibers due to its lowest dielectric constant.

While making comparison with nanofiber diameters of P(BA-co-MMA) copolymer and P(BA-co-MMA)/PPy composites. It was clearly seen that nanofiber diameters were strongly dependent on pyrrole content in composites. Nanofiber diameters of P(BA-co-MMA) copolymer was 600 nm. Mole percent of the initially added Py concentration varies from 10% to 40%, the average diameters of the nanofibers were reduced from 463 to 263 nm. The diameters of the fibers decrease slightly with the increase of Py feed ratio in composition. With the increase of the initially added Py concentrations, some beads begin to appear. This may be a result of the increased PPy content in the electrospinning solutions and also decrease in viscosity. The hydrophobicity seems to be related to the surface morphology. P(BA-co-MMA) copolymer had contact angle with water as 152^{o}, by addition pyrrole on the compostites hydrophobicity would become greater. By DMA, thermal effect of PPy on the copolymer structure was investigated. Decrease in glass transition temperatures with increasing feed pyrrole ratio were lead to lack of chain flexibility of polymer. DMA also revealled that the brittleness of PPy caused decrease in tensile

strength of polymer films. Lastly, electrical conductivity measurements were investigated. The increase in the A.C. electrical conductivity of the P(BA-co-MMA)/PPy composites also a linear increasing relationship was obtained between absorbance values of CH plane vibration of PPy.

REFERENCES

[1] Frushour, B. G., and Knorr, R. S.; 1998: *Handbook of Fiber Chemistry, 2nd* ed., pp. 875, Eds. Lewin M., Marcel Dekker, New York.

[2] Nuyken, O.; 1992: *Handbook of Polymer Synthesis, Part A*, pp. 277, Eds. Kricheldorf H.R., New York.

[3] Rulison, C.; 1998: *Water Soluble Polymers, Solution Properties and Applications*, pp. 6, Eds. Amjad Z., Plenum, New York.

[4] Kim, J.H., Kim, K.Y.; 1987: Permeation Characteristics of Solutes through Water Swollen Polymeric Membranes: II. Copoly(acrylonitrile-acrylic acid) Membranes. *Polymer(Korea)*. Vol.**11**, pp. 71-80.

[5] Cristallini, C., Ciardelli, G., Barbani, N., Giusti, P.; 2004: Acrylonitrile-Acrylic Acid Copolymer Membrane Imprinted with Uric Acid for Clinical Uses. *Macromoecular Bioscence*. Vol.**4**, pp. 31-38.

[6] Shan, J. D., He, Y., Wang, S., Xue, H., Zheng, H.; 2006: A Porous Poly(acrylonitrile-co-acrylic acid) Film-based Glucose Biosensor Constructed by Electrochemical Entrapment. *Analytical Biochemistry*. Vol.**356**, pp. 215-221.

[7] Wang, H.Y., Kobayashi, T., Fujii, N.; 1996: Molecular Imprint Membranes Prepared by the Phase Inversion Precipitation Technique. *Langmuir*. Vol.**12**, pp. 4850-4856.

[8] Aqil, A., Detrembleur, C., Gilbert, B., Jerome, R., Jerome, C.; 2007: Controlled RAFT Synthesis of Polyacrylonitrile-*b*-poly(acrylic acid) Diblocks as Precursors of Carbon Nanocapsules with Assistance of Gold Nanoparticles. *Chem. Mater.* Vol.**19**, pp. 2150-2154.

[9] Moghadam, S.S., Bahrami, S.H.; 2005: Copolymerization of Acrylonitrile-Acrylic Acid in DMF-Water Mixture. *Iranian Polymer Journal*. Vol. **14** , pp. 1032-1041.

[10] Shan, D., Cheng, G., Zhu, D., Xue, H., Cosnier, S., Ding, S.; 2009: Direct Electrochemistry of Hemoglobin in Poly(acrylonitrile-*co*-acrylic acid) and Its Catalysis to H_2O_2. *Sensors and Actuators B.* Vol.**137**, pp. 259-265.

[11] Brar, A.S., Dutta, K.; 1998: Microstructure and Compositional Sequence Determination of Acrylonitrile/Acrylic acid Copolymers by NMR Spectroscopy. *European Polymer Journal*. Vol.**34**, pp. 1585-1597.

[12] *Encyclopædia Britannica, Inc.1997*

[13] Kumar, D., Sharma, R.C.; 1998: Advances in Conductive Polymers. *European Polymer Journal*. Vol.**34** , pp. 1053-1060.

[14] Wang, L.X., Li, X.G., Yang, Y.L.; 2001: Preparation, Properties and Applications of Polypyrroles, *Reactive and Functional Polymers*. Vol.**47**, pp. 125-139.

[15] Lee, C.Y., Lee, D.E., Joo, J., Kim, M.S., Lee, J.Y., Jeong, S.H., Byun, S.W.; 2001: Conductivity and EMI Shielding Efficiency of Polypyrrole and Metal Compounds Coated on(non) Woven Fabrics Synthetic Metals, Vol.**119**, pp. 429-430.

[16] Roncali j., 1999, Electrogenerated Funct., "Conjugate polymers as advanced electrode materials", Journal of Materials Chemistry, 1875-1893.

[17] Gencturk A., 2007, "Electropolymerization and Characterization of 1-(4-Methylphenyl)-1H-Pyrrole and 2,2-Dimethyl-3,4-Propylenedioxy Thıophene, Istanbul Technical University, 4-7.

[18] Unlu H. (1992). "A Thermodynamic Model for Determining Pressure and Temperature Effects on the Bandgap Energies and other Properties of some Semiconductors". Solid State Electronics 35 (9): 1343–1352.

[19] James D. M., Christoph W., Macromol., Increased Electrical Conductivity in Poly(3,4- ethylenedioxythiophene) upon Cross-Linking Chem. Phys.", 2008, 209, 1959–1966,WILEY-VCH Verlag GmbH & Co. KGaA, Weinheim

[20] Ross, S (1961). "Faraday Consults the Scholars: The Origins of the Terms of Electrochemistry". Notes and Records of the Royal Society of London (1938–1996)

[21] Heeger, A. J., Schrieffer, J. R., and Su, W. P., 1998: Soliton Excitations in Polyacetylene, *Physical Review B*, **22**, 2099-2111.

[22] http://www.google.com.tr/imgres?imgurl=http://www.globalspec.com/RefArticleImages/

[23] Capaccioli, S., Lucchesi, M., Prevesto, D., and Rolla, P. A., 2004: Inter-Chain and intra-chain Hopping Transport in Conducting Polymer, *Physica Status Solidi (c)*, **1**, 148-151.

[24] Briad, J. L., Chance, R. R., and Silbey, R., 1981: Theoretical Studies of Charge Defect States in Doped Polyacetylene and Polyparaphenylene, *Molecular Crystals and Liquid Crystals*, **77**, 319-332.

[25] Li, X. G., Yang, Y. L., and Wang, L. X., 2001: Preparation, Properties and Applications of Polypyrroles, *Reactive & Functional Polymers*, **47**, 125-139.

[26] Efimov, O. N., and Vernitskaya, T. V., 1997: Polypyrrole: A Conducting Polymer; Its Synthesis, Properties and Applications, *Russian Chemical Reviews*, **66**, 443-457.

[27] Börüban,Ç., 2007: Synthesis and chracterization of polypyrole-montmorillonite and polypyrrole-polypropylene composites, *M.S.c Thesis*, Middle East Technical University, Ankara, Türkiye.

[28] Baytekin, S., 2009: Synthesis and chracterization of polypyrrole nanoparticles and their nanocomposites with polypropylene, *M.S.c Thesis*, Middle East Technical University, Ankara, Türkiye.

[29] De, A., and Gangopadhyay, R., 2000: Conducting Polymer Nanocomposites: A Brief Overview, *Chemistry of Materials*, **12**, 608-622.

[30] Li, X. G., Yang, Y. L., and Wang, L. X., 2001: Preparation, Properties and Applications of Polypyrroles, *Reactive & Functional Polymers*, **47**, 125-139.

[31] Efimov, O. N., and Vernitskaya, T. V., 1997: Polypyrrole: A Conducting Polymer; Its Synthesis, Properties and Applications, *Russian Chemical Reviews*, **66**, 443-457.

[32] Baykal, L., (2007). M. Sc. Thesis, *Istanbul Technical University*.

[33] Sukigara S., Gandhi M., Ayutsede J., Micklus M., Ko F., (2003). Regeneration of Bombyx mori silk by electrospinning—part 1:processing parameters and geometric properties. Polymer;44:5721–7.

[34] Russo P. , 2008, Intrinsic Viscosity Documents, 1-10

[35] McKee M., G., Layman J., M., Cashion M., P., (2006). Long TE. Phospholipid non-woven electrospin membranes. Science; 311:353–5

[36] Burger C., Hsiao B., S., Chu B., (2006). Nanofibrous marterials and their applications. Annu Rev Mater Res; 36:333–68

[37] Hohman M., M., Shin M., Rutledge G., Brenner M., P., (2001). Electrospinning and electrically forced jets. II. Applications. Phys Fluids;13:2221–36.

[38] Fong H., Chun I., Reneker D., H., (1999). Beaded nanofibers formed during electrospinning, Polymer;40:4585–92

[39] Zhang C., Yuan X., Wu L., Han Y., Sheng J., (2005). Study on morphology of electrospun poly (vinyl alcohol) mats. Eur Polym J;41:423–32

[40] http://depts.washington.edu/eooptic/linkfiles/dielectric_chart[1].pdf.

[41] Baker, S. C., Atkin, N., Gunning, P. A., Granville, N., Wilson, K., Wilson, D., Southgate, J., (2006). Characterisation of electrospun polystyrene scaffolds for three-dimensional in vitro biological studies, *Biomaterials*, vol.27, pp. 3136-6146

[42] Megelski S., Stephens J., S., Chase D., B., Rabolt J., F., (2002). Micro-and nanostructured surface morphology on electrospun polymer fibers. Macromolecules;35:8456–66

[43] Kumbar S., G., Nukavarapu S., P., James R., Hogan M., V., Laurencin C., T., (2008). Recent patents on electrospun biomedical nanostructures: an overview. Biomed Eng 2008;1: 68–78.

[44] Ajayan P. M., Schadler, L. S. and Braun, P. V., (2003). Nanocomposite Science and Technology, Weinheim, Wiley-VCH

[45] Avcı, M. Z., (2011), Electrospun Nanofibers of Methyl Methacrylate and Butyl Acrylate Copolymers, ITU M.S. thesis.

[46] Cetin S., Karakas H., Ciobanub R., Olariub M., Kaya N.U., Unsal C., Kalaoglu F., Sarac A. S., (2010). Polymerization of pyrrole derivatives on polyacrylonitrile matrix, FTIR–ATR and dielectric spectroscopic characterization of composite thin films, Synthetic Metals, 160 1189–1196

[47] Cetin S., Kalaoglu F., Karakas H., F., Sarac A. S., (2011). Dielectric, FTIR Spectroscopic and Atomic Force Microscopic Studies on Polypyrrolepoly (acrylonitrile-co-vinyl acetate) Composites, Polymer Composites.

[48] Manuela M., Raposoa M., Ana M., Maurício C., Kirschb G., (2004), Synthesis and UV-visible properties of thienyl- substituted pyrrole azo dyes, ECSOC

[49] Cetin S., Kalaoglu F., Karakas H., F., Sarac A. S., (2010). Electrospun Nanofibers of Polypyrrole-Poly(Acrylonitrile-*co*-Vinyl Acetate, Textile Research Journal, Vol 80 (17): 1784–1792

[50] Yanılmaz, M., Erbay, B.T.,Serhatlı, E., Saraç, A.S., (2012). Synthesis of Urethane Acrylate based Electromagnetic Interference, *Journal of Applied Polymer Science*, DOI: 10.1002/APP.38094

[51] Balkan T., Sarac A. S., (2011). Synthesis and Characterization of Electrically Conductive Composite Films of Polypyrrole /Poly(Acrylonitrile-co-Styrene), Fibers and Polymers, Vol.12, No.5, 565-571

[52] Cetin S., Kalaoglu F., Karakas H., F., Sarac A. S., (2011)., Characterization of Conductive Poly(Acrylonitrile-co-Vinyl Acetate) Composites: Matrix Polymerization of Pyrrole Derivatives, Fibers and Polymers 2011, Vol.12, No.2, 151-158

CURRICULUM VITAE

Name Surname: Derya AKÇÖREN

Place and date of birth: Ankara - 02.06.1986

Address: Boğaziçi C Sitesi C-6 Daire:3, Poligon Mah. – Sarıyer/İSTANBUL

E-mail: deryaakcoren@gmail.com

B.Sc.: Gazi University - Chemical Engineering

M.Sc.: Istanbul Technical University - Polymer Science and Technology

PUBLICATIONS/PRESENTATIONS ON THE THESIS

- **ÇETECİOĞLU, D., BALKAN, T, SARAC, A.S.,** 2011: Electrografting Of Poly(n-vinylcarbazole) And Poly(n-vinylcarbazoleco-styrenesulfonic Acid Sodium Salt): Cyclovoltammetric And Morphological Study, *NanoTR VII 2011 - Nanoscience and Nanotechnology Conference*, June 2011, Istanbul, TURKEY